Spring 2015

# Optical properties of black silicon - an analysis

Suramya Sekhri
*New Jersey Institute of Technology*

# Copyright Warning & Restrictions

The copyright law of the United States (Title 17, United States Code) governs the making of photocopies or other reproductions of copyrighted material.

Under certain conditions specified in the law, libraries and archives are authorized to furnish a photocopy or other reproduction. One of these specified conditions is that the photocopy or reproduction is not to be "used for any purpose other than private study, scholarship, or research." If a, user makes a request for, or later uses, a photocopy or reproduction for purposes in excess of "fair use" that user may be liable for copyright infringement,

This institution reserves the right to refuse to accept a copying order if, in its judgment, fulfillment of the order would involve violation of copyright law.

Please Note: The author retains the copyright while the New Jersey Institute of Technology reserves the right to distribute this thesis or dissertation

Printing note: If you do not wish to print this page, then select "Pages from: first page # to: last page #" on the print dialog screen

**ABSTRACT**

**OPTICAL PROPERTIES OF BLACK SILICON- AN ANALYSIS**

**by**

**Suramya Sekhri**

Silicon is the preeminent solar cell material of the day because it is the first semiconductor that was learned to commercialize and continues to be the principal semiconducting material used in photovoltaic technology for the manufacture of solar cells. Silicon, an indirect band gap semiconducting material, has a reflectance of about 30% in the visible range of wavelengths. Standard Silicon solar cells are not entirely useful in the infrared spectrum region. In order to enhance the performance of Silicon solar cells, reflectance losses must be minimized and absorption must be maximized. In the solar cell industry, anti-reflection (AR) coating is used to suppress reflection losses. AR coatings are limited in use because they only reduce the reflectance for a narrow range of wavelengths and incident angle since their functionality is based on a quarter-wavelength coating. Surface texturing is a technique, by which the reflectivity is reduced. Black Silicon is a material with surface roughness in the micron scale. Black Silicon, when used instead of Crystalline Silicon, offers the possibility to increase the absorption of light in the visible and infrared range of wavelengths. Black Silicon has a very low reflectivity in the visible range of wavelengths. It exhibits high absorptance in the visible and infrared region. The main objective of this thesis is to study the various fabrication techniques used to form Black Silicon, present a comparative study of

structural differences and analyze its optical properties by simulation and compare them with the simulated and experimental optical properties of Black Silicon and Crystalline Silicon.

# OPTICAL PROPERTIES OF BLACK SILICON- AN ANALYSIS

**by**
**Suramya Sekhri**

**A Thesis**
**Submitted to the Faculty of**
**New Jersey Institute of Technology**
**in Partial Fulfillment of the Requirements for the Degree of**
**Master of Science in Materials Science and Engineering**

**Interdisciplinary Program in Materials Science and Engineering**

**May 2015**

**APPROVAL PAGE**

**OPTICAL PROPERTIES OF BLACK SILICON- AN ANALYSIS**

**Suramya Sekhri**

---

Dr. N. M. Ravindra, Thesis Advisor — Date
Professor, Department of Physics, NJIT
Director, Interdisciplinary Program in Materials Science & Engineering, NJIT

---

Dr. Michael Jaffe, Committee Member — Date
Research Professor, Department of Biomedical Engineering, NJIT

---

Dr. Halina Opyrchal, Committee Member — Date
Senior University Lecturer, Department of Physics, NJIT

---

Mr. B. S. Mani, Committee Member — Date
University Lecturer, Department of Mechanical & Industrial Engineering, NJIT

---

Dr. Willis B. Hammond, Committee Member — Date
CEO, W. B. Hammond Associates, LLC

## BIOGRAPHICAL SKETCH

**Author:** Suramya Sekhri

**Degree:** Master of Science

**Date:** May 2015

**Undergraduate and Graduate Education:**

- Master of Science in Materials Science and Engineering,
  New Jersey Institute of Technology, Newark, NJ, USA, 2015

- Bachelor of Science in Physics,
  Kirori Mal College, University of Delhi, Delhi, India, 2013

**Major:** Materials Science and Engineering

To the five pillars of my life: God, my Grandparents, and my Parents.

Without you, my life would fall apart.

I might not know where the life's road will take me,

but walking with You, God, through this journey has given me strength.

Mom, you have given me so much, thanks for your faith in me,

and for teaching me that I should never surrender.

Daddy, you always told me to "reach for the stars." I think I got my first one.

Thanks for inspiring me for everything in life and of course, Physics!

**ACKNOWLEDGEMENTS**

I would like to express my deepest appreciation to my thesis advisor Dr. N.M. Ravindra who has the attitude and substance of a genius. He continually and convincingly conveyed a spirit of adventure in regard to my thesis and research. Without his guidance and persistent help this thesis would not have been possible. Thanks for giving me the opportunity to be part of the Black Silicon research.

Special thanks to all my thesis committee members Dr. Michael Jaffe, Dr. Halina Opyrchal, Mr. B. S. Mani, Dr. Willis B. Hammond for their valuable time and for serving on my committee.

Special Thanks to Ms. Clarisa Gonzalez, Associate Director of Graduate Studies and Ms. Lillian Quiles, Administrative Assistant at the Graduate Studies Office for their valuable and effective inputs and helping me improve my overall thesis.

I am grateful to all my research group members: Sita Laxmi, Chiranjivi Lamsal, Vishal Nakhate, Aniket Maske, Sarang Muley who have supported me throughout entire process, both by keeping me harmonious and helping me putting pieces together.

I am highly gratified by my Grandparents: Mr. Madan Lal Sekhri and Mrs. Sudesh Sekhri and parents: Mr. Vikram Sekhri and Mrs. Anu Sekhri for their limitless and immense support, encouragement and blessings. Thank you for always boosting my morale and keeping faith in me. I appreciate my sibling: Rohinya Sekhri's never- ending belief in me and for being there through thick and thin. My deepest gratitude to my

friends back in India for always keeping my spirits high and for all the encouragement and praise.

**TABLE OF CONTENTS**

**TABLE OF CONTENTS**
**(Continued)**

**TABLE OF CONTENTS**
**(Continued)**

**Chapter** **Page**

## LIST OF TABLES

## LIST OF FIGURES

**LIST OF FIGURES**
**(Continued)**

**LIST OF FIGURES**
**(Continued)**

**LIST OF FIGURES**
**(Continued)**

# CHAPTER 1

# INTRODUCTION

Silicon is a word commonly acknowledged by everyone, at least in the phrase "Silicon Valley," home to many of the world's largest high tech corporations, as well as thousands of tech startup companies, large number of Silicon chip innovators and manufacturers. Silicon is the element to thank for the computer which is used by almost every individual in today's world [18]. A crucial component in microelectronics and computer chips, this extremely common element is also responsible for warm, white beaches — silica, an oxide of Silicon, which is the most common component of sand. Silicon is the seventh-most abundant element in the universe and the second-most abundant element on the planet, after oxygen [30]. The earth is constructed of Silicon, and it is used every day in the form of glass and pottery. What carbon is to the living world, Silicon is to the non-living.

Crystalline Silicon is a primary component in the most common type of solar cells. A band gap of 1.17 eV helps in efficient detection of visible light and conversion of sunlight into electricity [31]. One of the most promising alternatives to fossil fuels for electricity is solar power. Easily integrated with other microelectronics, Silicon is used in many forms (including crystalline, amorphous, and porous) in numerous optoelectronic devices. Having a large thermal conductivity and large high-field drift velocity, Silicon is one of the most advantageous semiconductor materials [18]. One of the main reasons that Silicon is the semiconductor material of choice in microelectronics is that it forms a

unique oxide on the surface when heated to high temperatures. This facilitates device fabrication for two reasons [30]:

(1) It neutralizes defects on the Silicon surface

(2) It allows for straightforward planar processing

However, it has certain shortcomings. As an indirect band-gap material, it is a poor light emitter. Silicon cannot be used to detect many important communications wavelengths. Also, Silicon solar cells fail to convert nearly a third of the sun's spectrum into electricity [55]. The efficiency of the photovoltaic devices and photo-electronic detectors made from Crystalline Silicon decreases seriously due to its high reflectivity to the visible and near infrared light [56].

In order to overcome the intrinsic disadvantages of Silicon, many approaches have been explored. Main motive is to reduce the reflectivity and transmissivity resulting in increased absorptance. The two possible methods to obtain required results fall under two categories [45]:

1) Anti-reflection coating

2) Light-trapping structure

Among these methods, the first method is relatively more expensive than the latter and since surface texturing is a more permanent and effective solution to decrease reflections, a technique is employed to obtain needle-shaped surface structure, which is simply a surface modified microstructure of Silicon, called the Black Silicon. Without any

doping, the absorption of Black Silicon can be raised to over 90% in ultraviolet and visible range [3, 4]. There are different processes to fabricate Black Silicon, including reactive ion etching (RIE), electrochemical etching, acid etching, Mazur's method etc.

The renewable energy industry has come a long way in relatively little time. The costs of renewable technologies continue to go down, while renewable capacities at many utilities continue to go up [3, 4]. Black Silicon is an active candidate in renewable energy area due to its major application in solar cells. There have been studies that show about 18.2% [49] increase in efficiency of the black Silicon solar cells. Black Silicon has been successfully identified in making cheaper, more sensitive light detectors and imaging devices, while potentially taking advantage of established Silicon manufacturing methods.

This thesis basically gives the detailed understanding of the optical properties like Reflectance, Transmittance and Absorptance of Black Silicon as well the various ways in which it is formed. Also, the calculations and graphical interpretations prove the rise in Absorptance and gradual decrease in Reflectance and Transmittance which is the basic purpose of the thesis. Data interprets Effective refractive index of Black Silicon to be lower than that of Crystalline Silicon and the extinction coefficient higher that of Crystalline Silicon. And finally, its impact and usefulness in the solar industry and other areas of research have been prospected.

# CHAPTER 2

# SILICON- AN ANALYSIS

## 2.1 Natural Abundance

In one's perspective, human beings have always used SILICON. On being the second most abundant element in the Earth's crust and eighth most abundant element in the universe, Silicon occurs mostly in form Silicon dioxide as in combination with oxygen and several metals and also, in silicate form but is never found in free form i.e., it's never found isolated [31]. It is always combined with one or more other elements as a compound. Nearly every naturally occurring rock or mineral contains some Silicon. In fact, Silicon was also being used when ancient people built clay huts or sandstone structures [30-33]. Silicon has also been detected in the Sun and stars. It also occurs in certain types of meteorites known as aerolites or "stony meteorites [18]."

Two allotropes of Silicon exist at room temperature: Amorphous and Crystalline.

### 2.1.1 Amorphous Silicon

It appears as a brown powder and suffers from lower electronic properties which make it flexible in its applications. It is widely used as an active layer in thin film transistors (TFTs) and mainly for liquid display crystal (LCDs) [13]. Amorphous Silicon is also used as a photovoltaic solar cell material. Due to its lower efficiency than Crystalline Silicon solar cells, it can also be used in materials which require very little power [30]. But mainly

their thinness or flexibility makes it to the list of advantages. The Figures 2.1, 2.2, 2.3 illustrates the atomic packing structures of Silicon allotropes.

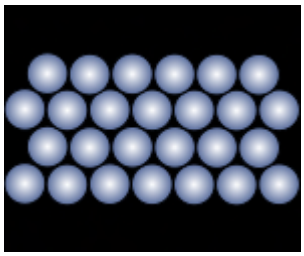

**Figure 2.1** Monocrystalline Silicon [18].

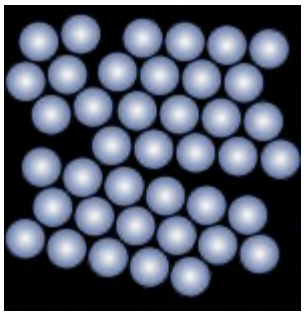

**Figure 2.2** Polycrystalline Silicon [18].

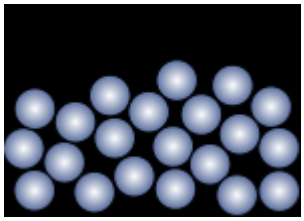

**Figure 2.3** Amorphous Silicon [18].

### 2.1.2 Crystalline Silicon

It has a metallic luster and a grayish color. Single crystals of crystalline Silicon can be grown with a process known as the Czochralski process [33]. In this process Silicon crystals, when doped with elements such as boron, gallium, germanium, phosphorus or arsenic, are used in the manufacture of solid-state electronic devices, such as transistors, solar cells, rectifiers and microchips. Crystalline Silicon is basically used in traditional, conventional, wafer-based solar cells. Two of its crystalline forms include- multicrystalline Silicon and monocrystalline Silicon [21]. These are the two dominant semiconducting materials used in photovoltaic technology for the production of solar cells.

## 2.2 History

Silicon as an element came to existence only after the nineteenth century [19]. Then, a number of chemists tried to separate Silicon from the other elements with which it was combined in the Earth. English scientist Sir Humphry Davy (1778-1829) developed a technique for separating elements that tightly bonded [38]. He melted these compounds and passed an electric current through them. The technique was successful for producing free or elemental sodium, potassium, calcium, and a number of other elements for the first time. But that method was a fail with Silicon and couldn’t result in forming elemental Silicon.

### 2.2.1 First time preparation- 1823

Elemental Silicon was prepared for the first time in 1823 by Jöns Jacob Berzelius, a Swedish chemist, by heating chips of potassium in a silica container and then carefully washing away the residual by-products [31]. According to the technique, Silicon tetra fluoride ($K_2SiF_6$) was placed in the presence of warm potassium. However, it has been claimed that way before 1823, in 1809, Gay-Lussac and Thenard had already tried to obtain amorphous Silicon by applying the same method [38]. The substance obtained in 1823, by Berzelius was a purer product as a result of exhausting filtering. This pure Silicon was prepared from the reaction of potassium fluorosilicates with potassium [18].

### 2.2.2 Crystalline Silicon - 1854

In its crystalline form, Silicon was first prepared by Deville, in 1854, through the electrolysis of impure sodium-aluminum chloride with about 10% of Silicon [38]. At the beginning of the 20th century in 1907, the interaction of silica with the carbon was studied, which prepared the way to the process of obtaining Silicon for commercial purposes during the whole century [20].

### 2.2.3 Today's Scenario

Elemental Silicon today is commercially prepared by the heating of Silicon dioxide with coal in electrical furnaces. The Czochralski process [38] is commonly used to produce single crystals of Silicon which can be done by introducing a crystalline seed in melted Silicon by slowly lowering the temperature. Silicon producers reduce high-grade quartz

sand to elemental Silicon through a carbo-thermic smelting process [39, 40]. The formula for reducing sand to elemental Silicon is given by:

$$SiO_2 + 2C \longrightarrow Si + 2CO_{(g)} \qquad (2.1)$$

- This reaction occurs in an electric furnace at a temperature less than 1,400°C (<2,600°F) [38].
- The carbon monoxide gas leaves the furnace so the Silicon cannot react with the carbon to form Silicon dioxide [41].
- The molten elemental Silicon, which is about 99 percent pure, is then cooled and broken into lumps [41].

### 2.3 Occurrence

Silicon makes up 25.7% of the Earth's crust and is the second most abundant element on Earth, after oxygen. Pure Silicon crystals are only occasionally found in nature; they can be found as inclusions with gold and in volcanic exhalations [36]. Silicon is usually found in the form of Silicon dioxide (also known as silica), and silicate.

Silicon dioxide occurs in minerals consisting of pure Silicon dioxide in different crystalline forms. Sand, amethyst, quartz, rock crystal, chalcedony, flint, jasper, agate, and opal are some of the forms in which Silicon dioxide appears. The quartz is very common and it can be found in granite, sand and sandstone [18]. It is a piezoelectric substance that is used to stabilize amplifier circuits, to measure high electrical potentials (thousands of volts) or to measure high instantaneous pressures.

Silicon also occurs as silicates (various minerals containing Silicon, oxygen and one or another metal), for example feldspar [34]. These minerals occur in clay, sand and various types of rock such as granite and sandstone. Asbestos, feldspar, clay, hornblende, and mica are a few of the many silicate minerals.

As a whole, 60% of the terrestrial crust consists of silica and silicates. The $SiO_4$ is the primary structural unit of all these substances [35]. Actually, the silicates are a very extensive group of compounds, resulting from the combination of complex metallic ions or complex negative ions with $SiO_4$ units [36].

There are also several forms of amorphous silica with water, such as the opal or the geyserite. From these, the black opal of Australia stands out, being one of the most valuable precious stones [36].

## 2.4 Properties

### 2.4.1 Physical

Silicon is a metalloid, an element with properties of both metals and non-metals. Silicon has a hardness of about 7 on the Mohs scale of mineral hardness [20, 33]. The Mohs scale is a way of expressing the hardness of a material. It runs from 0 (for talc) to 10 (for diamond) [20]. Silicon is a semiconductor. A semiconductor is a substance that conducts an electric current better than a non-conductor—like glass or rubber—but not as well as a conductor—like copper or aluminum [18].

**Table 2.1** Physical Properties of Silicon [20]

| What are the Physical Properties of Silicon? | |
|---|---|
| Color | Pure Silicon is a hard, dark gray solid |
| Phase | Solid |
| Luster | A metallic shine or glow |
| Allotropic | Silicon has two allotropic forms, a brown amorphous form, and a dark crystalline form |
| Solubility | Soluble in hydrofluoric acid and alkalis |
| Melting point | Melts at 1417°C |
| Boiling point | Boils at 2600°C |
| Conductivity | It is a semi-conductor |

### 2.4.2 Chemical

Silicon is a relatively inactive element at room temperature. It does not combine with oxygen or most other elements. Water, steam, and most acids have very little effect on the element [32]. At higher temperatures, however, Silicon becomes much more

reactive. In the molten (melted) state, for example, it combines with oxygen, nitrogen, sulfur, phosphorus, and other elements. It also forms a number of alloys very easily in the molten state [20].

**Table 2.2** Chemical Properties of Silicon [20]

| **What are the Chemical Properties of Silicon?** | |
|---|---|
| Compounds | Silicon forms compounds with metals (silicide) and with non-metals |
| Oxidation | Combined with oxygen as silica (Silicon dioxide, $SiO_2$) or with oxygen and metals as silicate minerals. It is stable in air even at elevated temperatures owing to the formation of a protective oxide film [19] |
| Flammability | Dark-brown crystals that burn in air when ignited |
| Color | Is transparent to long-wavelength infra-red radiation [18] |
| Reactivity with acids | Dissolves only in a mixture of nitric acid and hydrofluoric acid |

## 2.5 Applications

### 2.5.1 Solar Industry

#### History of Silicon Solar Cell

The first photovoltaic effect (electricity generated by light) was observed in 1839 by Edmond Becquerel using wet chemistry [30]. Independently, Silicon was one of many materials used in radio equipment—a sharp metal point jabbed into unrefined Silicon

formed a crude version of a diode, an important element in radio receivers. These developments led to the accidental discovery of the Silicon solar cell in 1940 [30], when, at Bell Telephone Labs, when the photovoltaic effect in a half-purified bar of Silicon was observed by Russell Ohl [31]. Since then, research on the processing and physics of Silicon grew until the integrated circuit crystallized its role in history.

**Advantages**

Crystalline Silicon photovoltaic is the most widely used photovoltaic technology. Crystalline Silicon photovoltaics are modules built using crystalline Silicon solar cells, developed from the microelectronics technology industry. Crystalline Silicon solar cells have high efficiency. The highest energy conversion efficiency reported so far for research crystalline Silicon PV cells is 25% [66]. Standard industrial cells, however, remain limited to 15–18% with the exception of certain high-efficiency cells capable of efficiencies greater than 20% [30, 66].

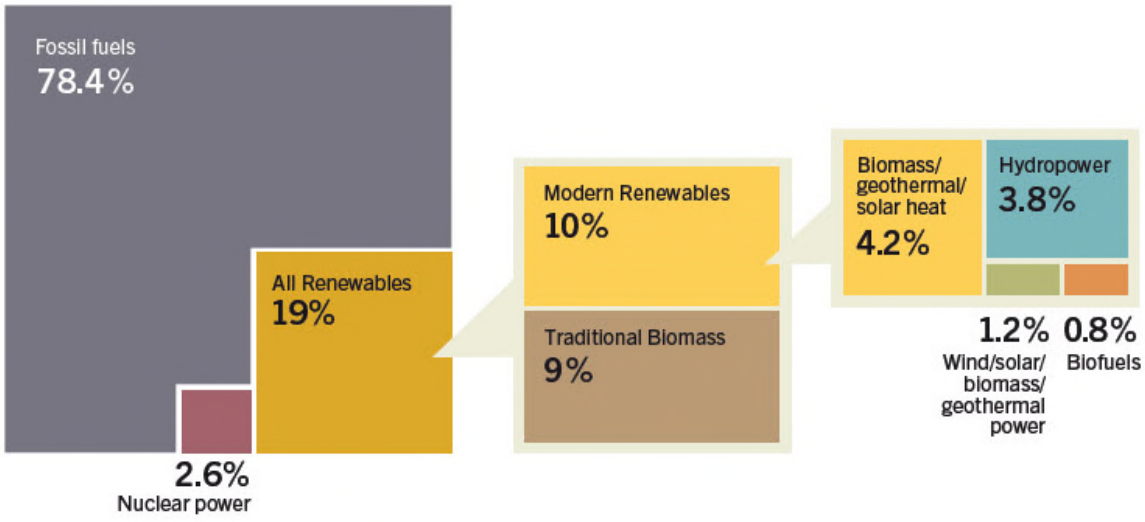


**Figure 2.3** Renewable Energy Share of Global Final Energy Consumption [22].

### 2.5.2 Electronics

One of the main reasons that Silicon is the semiconductor material of choice in microelectronics is that it forms a unique oxide on the surface when heated to high temperatures. This facilitates device fabrication for two reasons [30]:

1. It neutralizes defects on the Silicon surface
2. It allows for straightforward planar processing.

Semiconductors are able to manipulate electric current. They are used to rectify, amplify, and switch electrical signals and are thus integral components of modern day electronics. Semiconductors can be made out of a variety of materials, but the majority of semiconductors are made out of Silicon. But semiconductors are not made out of silicates, or silanes, or Silicones, they are made out pure Silicon that is essentially pure Silicon crystal [19].

### 2.5.3 Semiconductors

Semiconductors are unique materials that have neither the electrical conductivity of a conductor nor of an insulator. Semiconductors lie somewhere in between these two classes giving them a very useful property [18]. Semiconductors are able to manipulate electric current. They are used to rectify, amplify, and switch electrical signals and are thus integral components of modern day electronics.

Silicon lattice is essentially an insulator, as there are no free electrons for any charge movement, and is therefore not a semiconductor. This crystalline structure is

turned into a semiconductor when it is doped. Doping refers to a process by which impurities are introduced into ultra-pure Silicon, thereby changing its electrical properties and turning it into a semiconductor [32]. Doping turns pure Silicon into a semiconductor by adding or removing a very small amount of electrons, thereby making it neither an insulator nor a conductor, but a semiconductor with limited charge conduction. Subtle manipulation of pure Silicon lattices via doping generates the wide variety of semiconductors that modern day electrical technology requires [19].

Semiconductors are made out of Silicon for two fundamental reasons [21]:

- Silicon has the properties needed to make semiconductors
- Silicon is the second most abundant element on earth.

### 2.5.4 Glasses

Glass is another Silicon derivate that is widely utilized by modern day society. If sand, a silica deposit, is mixed with sodium and calcium carbonate at temperatures near 1500 degrees Celsius [21], when the resulting product cools, glass forms. Glass is a particularly interesting state of Silicon. Glass is unique because it represents a solid non-crystalline form of Silicon [19].

The end result of this unique chemical structure is the often brittle typically optically transparent material known as glass. This silica complex can be found virtually anywhere human civilization is found [20].

Glass can be tainted by adding chemical impurities to the basal silica structure. The addition of even a little $Fe_2O_3$ to pure silica glass gives the resultant mixed glass a distinctive green color [35].

### 2.5.5 Ceramics

Silicon plays an integral role in the construction industry [18]. Silicon, specifically silica, is a primary ingredient in building components such as bricks, cement, ceramics, and tiles [31].

Additionally, silicates, especially quartz, are very thermodynamically stable. This translates to Silicon ceramics having high heat tolerance. This property makes Silicon ceramics particularily useful from things ranging from space ship hulls to engine components.

### 2.5.6 Fiber Optics

Modern fiber optic cables must relay data via undistorted light signals over vast distances. To undertake this task, fiber optic cables must be made of special ultra-high purity glass. The secret behind this ultra-high purity glass is ultra-pure silica [19, 20]. To make fiber optic cables meet operational standards, the impurity levels in the silica of these fiber optic cables have been reduced to parts per billion. This level of purity allows for the vast communications network that our society has come to take for granted [21].

### 2.5.7 Polymers

Silicone polymers represent another facet of Silicon's usefulness. Silicone polymers are generally characterized by their flexibility, resistance to chemical attack, impermeability to water, and their ability to retain their properties at both high and low temperatures. This array of properties makes Silicone polymers very useful. Silicone polymers are used in insulation, cookware, high temperature lubricants, medical equipment, sealants, adhesives, and even as an alternative to plastic in toys [18-22, 27].

**But Does/Will Silicon Continue To Be The Most Preferred Semiconductor For Applications In Solar Industry?**

Below given are the certain disadvantages of Silicon that helps us realize that we need to bring a revolutionary change to the Silicon surface to obtain an even better material with improves its overall properties.

MAJOR DRAWBACKS:

- Indirect band-gap nature ⇨ Poor light emitter
- Unable to detect many important communication wavelengths
- Silicon solar cells decline to convert (1/3) suns' spectrum into electricity
- Elemental Silicon is an inert material, Silicon dioxide is a potent respiratory hazard

- When certain conditions exist:

  Silicone + metal ions ⟹ high resistive films such as sodium silicate

❖ Crystalline solar cells - loopholes

  - High temperature and energy intensive manufacturing process
  - Use a relatively large amount of Si
  - Expensive
  - Fragile
  - Low band-gap (1.17 eV ~ 1060 nm)

- Thin film solar cells – shortcomings

  - Far less efficient
  - Require nearly twice as much space for the same amount of power
  - Shorter lifetime

Therefore, we introduce **BLACK SILICON**, simply a textured material that grows on Silicon which overcomes all the listed defects in Silicon.

# CHAPTER 3

# BLACK SILICON

## 3.1 Black Silicon History

| Year | Discovery |
|---|---|
| **1970s** | • Since, Silicon worked well as a semiconductor, the high natural reflectivity of the material greatly affected the efficiency of the Silicon cells [18].<br>• A clever way to overcome the natural reflectivity was to manipulate the surface of the Silicon on the nano scale [7].<br>• That could be done by altering the surface of the Silicon to obtain series of peaks and valleys and valleys, which greatly increased the absorption as incident photons were reflected into the peaks and absorbed by the material [15].<br>• This was theorized by Richard Stephens and George Cody [45].<br>• The reflectivity of a material greatly decreased by light trapping by multiple reflections [45]. |
| **1990s** | • Methods of Svetoslave Koynov, Martin Brand and Martin Stutzmann at the University of Munich were able to achieve an averAge reduction of surface reflection to about 8% - 15% [45].<br>• They used a wet etching process that utilized gold atoms to deform the surface of the Silicon [42].<br>• The method created a Silicon that survived the harsh chemical and thermal treatments during solar cell processing [43]. |
| **1999** | • Harvard University group, led by Eric Mazur developed a process in which black Silicon was produced by irradiating Silicon with femtosecond laser pulses in the presence of sulphur hexafluoride [9.]<br>• These spikes improved the absorption by increasing the self-reflection of light [9]. |

### 3.2 Production Process

The key to production of black Silicon is by developing methods of morphing the surface of the material that are economical and easily applicable for mass production. Further the surface produced must maintain its features as it is further manipulated and processed into a solar cell [4]. Over recent decades, a range of Black Silicon fabrication processes has been developed. In this section, the major techniques are reviewed.

### 3.3 Methods of Fabricating Black Silicon

The preparation methods for the fabrication of Black Silicon may be divided into dry and wet etching. The former involves gaseous reagents while the latter uses solution chemistry.

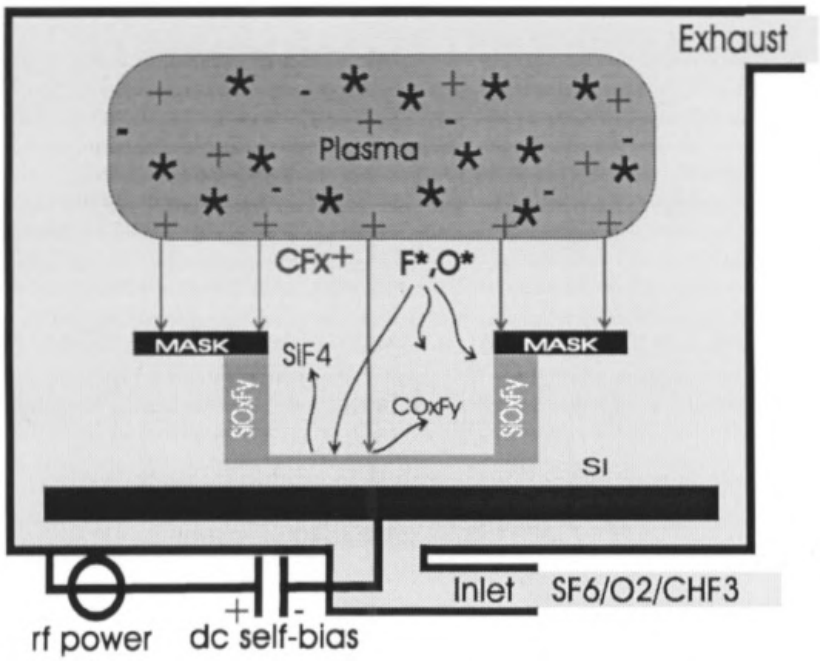


**Figure 3.1** Experimental setup to perform RIE [48].

### 3.3.1 Dry Etching:

**Experimental Set**

Black Silicon was first prepared by Reactive- ion etching (RIE) [43]. The reactive ion etching is used to form grass-like BSi. The use of reactive ion etching to form BSi surfaces was first reported by Jansen in 1995 [45]. Figure 3.1 shows the experimental set up used to perform RIE. This method employs $SF_6$ and $O_2$ gases to generate F* and O* radicals. F* is responsible for etching Silicon, producing volatile products such as $SiF_X$. These products, particularly $SiF_4$, react with O* to form a passivation layer of $SiO_XFy$ on a cooled Silicon substrate. This passivation layer is partly removed by ion bombardment and the exposed Silicon is further etched by F* [3, 4]. This process can be understood more precisely in Figure 3.2.

The etching reaction is exothermic, and reduces the chance of producing a new passivation layer since $SiOxFy$ is prone to desorption upon heating [13]. In contrast, there is far less ion bombardment on the side walls of the formed Silicon columns. So, the passivation layer there is largely preserved, preventing further etching. This etching/passivation mechanism leads to the formation of random Silicon micro structures with very high aspect ratios in a self-masking fashion F [48].

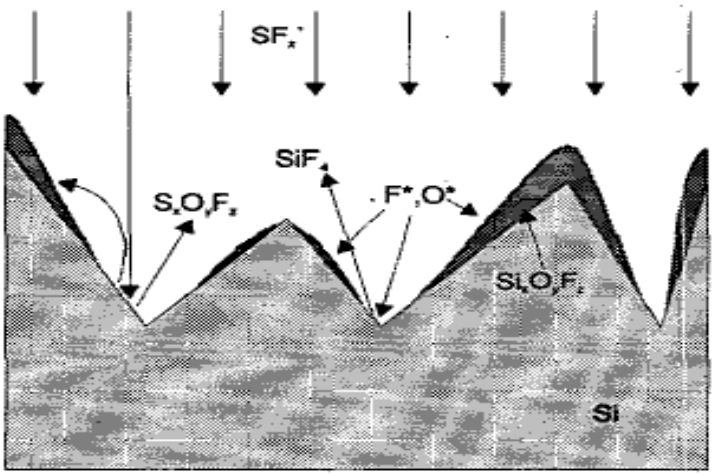


**Figure 3.2** Schematic Diagram Of The Formation Of Black Silicon Or Random Pyramids By RIE. Shaded Areas Are Si And F [7].

A further variation on RIE is the **Plasma Immersion Ion Implantation (PIII)** process. Like RIE, PIII uses $SF_6$ /$O_2$ gas combinations, $O_2$ and $SF_6$ gas is drained into the vacuum chamber at a flow rate [3]. During the PIII process, $SF_6$ and $O_2$ are ionized reactive ions and radicals. Under the negative voltage, the reactive ions are injected into the Silicon substrate to react with Silicon. After the PIII treatment, they are subjected to acid etching in 2% HCl and then in 10% HF to remove the contamination and oxides [4]. Then, the wafers are doped with phosphorous using with phosphorous oxychloride ($POCl_3$) as the dopant source at a diffusion temperature of 868°C [48].

On removal of phosphosilicate glass (PSG) layer from the diffused wafers surface with diluted HF (10% by volume), the wafers are subjected to edge etching [1]. Then Silicon nitride ($Si_3N_4$) layer for passivation is grown by plasma enhanced chemical vapor deposition process. Then the back electrode is fabricated by screen printing using Ag–Al paste [60, 67], Al paste and front side using Ag paste followed by baking and co-firing at

a proper temperature. Below is a flowchart which clearly explains the complete process of PIII [1, 3, 4].

**Table 3.2** Process Flow Chart Of Black Silicon Solar Cell Fabrication Process [1]

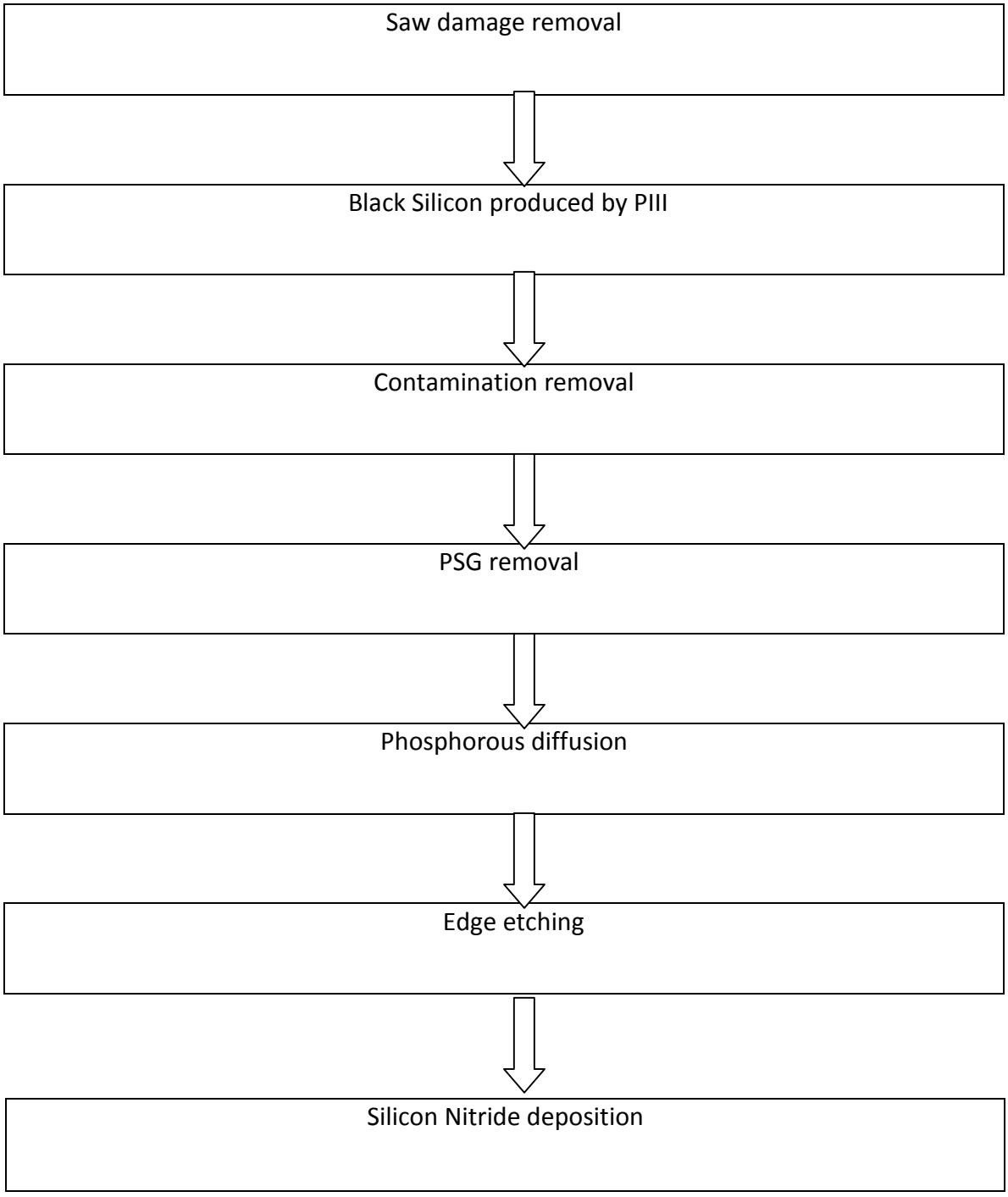

**Table 3.3** Process Flow Chart Of Black Silicon Solar Cell Fabrication Process(Continued) [1]

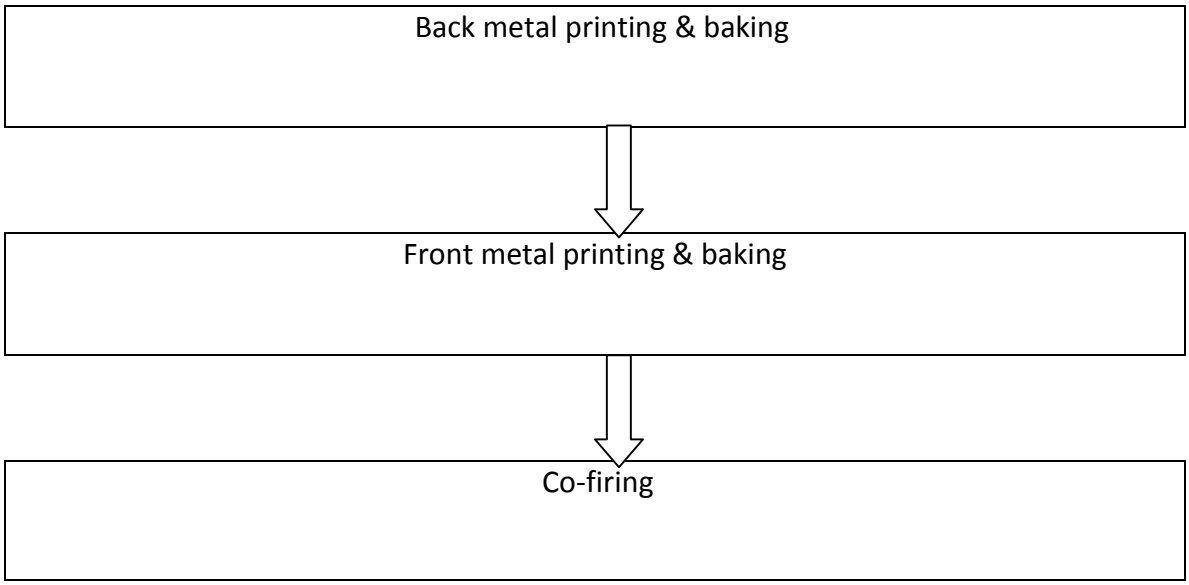


Another alternative reactive gas is $Cl_2$, which offers a lower etching rate in comparison to $SF_6/O_2$ but is much easier to manage [57], owing to the formation of nonvolatile by-products, and thus makes the control over the passivation layer deposition and Silicon etching comparatively straightforward [3, 4]. $Cl_2$ can also be added into $SF_6/O_2$ to enlarge the gas composition working window. Similarly, employing hydrogen bromide (HBr) and oxygen ($O_2$) during the plasma could enhance RIE [17]. During this process, bromide ions are primarily responsible for etching Silicon, resulting in the formation of $SiBr_4$. This reaction product can also react with O* radicals to form random distributed $SiBr_xO_y$ particles, acting as etching masks. Figure 3.3 explains the formation mechanism of needle-like structure by PIII process [1].

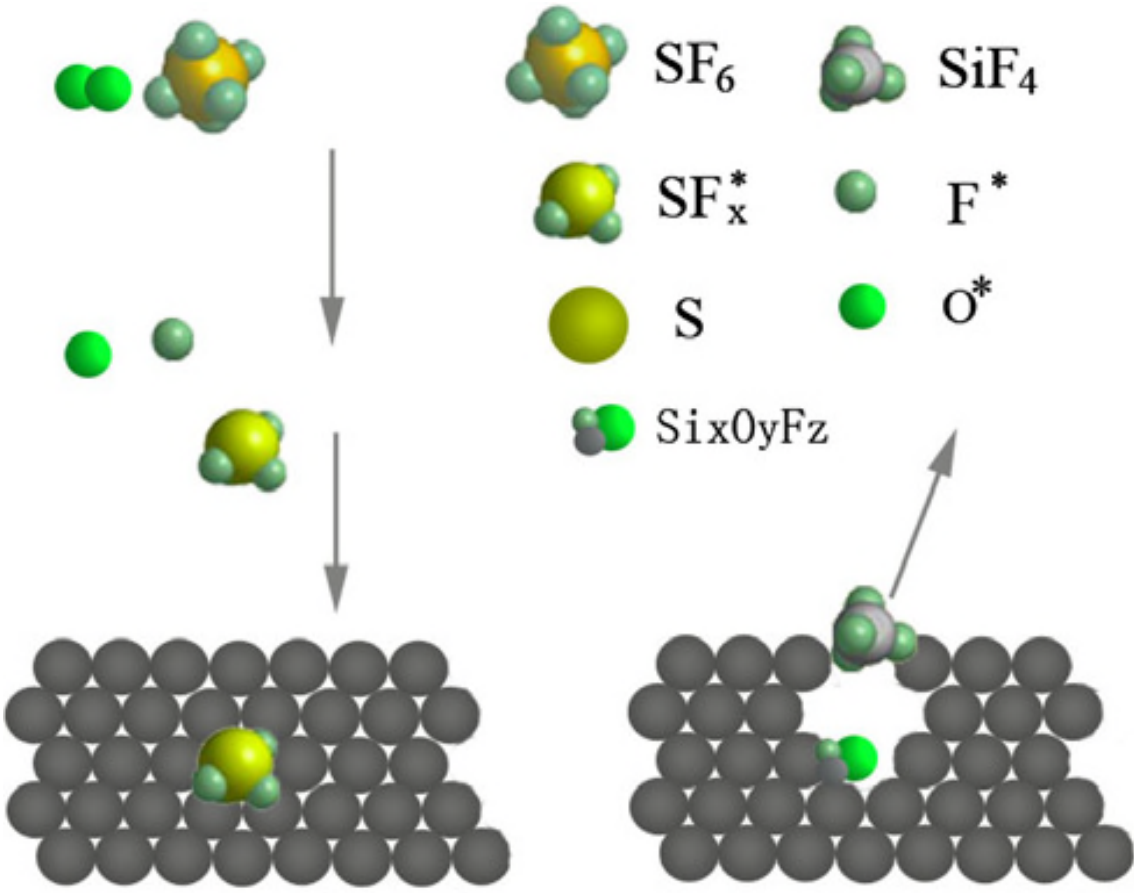


**Figure 3.3** The formation mechanism of needle-like structure by PIII process [1].

Apart from all other RIE mechanisms, another deep RIE, or Bosch, process, is also very popular where in $SF_6$ and $C_4F_8$ are alternatively introduced into the reaction chamber for etching and passivation, respectively [4]. By repeating this process for hundreds or even thousands of cycles, a very deep and near-vertical Silicon needle structure can be fabricated [50]. This two-step cycle process induces an undulating structure on the sidewalls of the Silicon needles, with an amplitude of several hundreds of nanometers, in contrast to the smooth side wall produced by cryogenic RIE [3].

### 3.3.2 Wet Chemical Etching

Wet chemical etching for preparing BSi includes both metal-assisted (metal catalyzed) chemical etching and electrochemical etching. Metal-assisted chemical etching (MACE) generally includes electroless metallization of the surface, or deposition of pre-made metal nanoparticles, followed by etching with a solution of containing an oxidant and a complexing agent for Silicon [3, 4]. MACE overcomes the disadvantages of dry etch techniques that need either expensive instruments and high energy consumption or complicated fabricating processes, making them unfavorable for industrial applications [7].

**Fabrication of Black Silicon Solar Cells – Metal Assisted Etching**

Silicon can be etched in the presence of HF and an oxidative agent, catalyzed by noble metals, to form micro-/nano-structured surfaces with various morphologies. In a typical etching process, a Silicon substrate is partly covered by noble metal nanoparticles, and immersed in a solution of HF and an oxidative agent [3]. Gold (Au) and silver (Ag) are the two most popular candidates since they can be deposited onto the surface under vacuum (i.e., via thermal evaporation, sputtering and electron beam evaporation) or in solution (i.e., via electroless deposition and electrodeposition) [4, 2]. This particular kind of Si etching, carried out at high dilution and in certain range of HF/oxidant concentrations [50,51].

In this process, noble metal nano particles are deposited as catalyst first and then an aqueous solution of HF and $H_20_2$ is used to etch Silicon. Here Ag assisted etching

has been adopted. Ag nano pores have been considered to be a potential candidate for light trapping in solar cells. This is mainly due to [2]:

1. Low absorption property

2. Powerful ability of coupling the incident light over a large angular range into the cells

This procedure includes p-type mc- Silicon pieces which are first soaked in alcohol, acetone and de-ionized water [2] in a sanitation bath for about 5 minutes respectively and then dipped into $HNO_3$-HF-$CH_3COOH$ mixed solution to remove any saw damage from the Silicon. Then BSi is fabricated by Ag catalyzed chemical etching in a polytertaflouroethylene container with 4.0 M HF and 0.01 M $AgNO_3$ mixture at the room temperature [2]. This is followed by removal of silver contamination on the Silicon surface by $HN0_3$ by a sanitation bath and rinsing with de-ionized water and then drying by blowing Nitrogen. Now after all these procedures a 30 nm $Sin_X$ layer is created on to the black Silicon surface [29].

In a basic metal assisted procedure, by electrloess deposition or vacuum technology, Silicon substrate is partly covered by a noble metal. Silicon beneath the noble metal is etched much faster than the one exposed to the solution due to catalysis [54]. As the process continues, the since the noble metals sinks below the surface this results in the formation of pores which depend on the initial morphology of the coverage by noble metal [2-4]. Since Ag had already been deposited electrolessly on substrate's surface when Silicon was immersed into the $AgNO_3$-HF solution [57]. Thus the main part of the electrochemical react is the electrochemical potential between

Silicon and Ag+/Ag. Reaction can be explained in two half-cell reactions given below [2, 4]:

Cathode Reaction:

$$Ag^{+} + e^{-}_{VB} \rightarrow Ag^{0}(s) \qquad (2.2)$$

Anode Reaction:

$$Si\ (s) + 2H_2O \rightarrow SiO_2 + 4H^{+} + 4\ e^{-}_{VB} \qquad (2.3)$$

$$SiO_2\ (s) + 6HF \rightarrow H_2SiF_6 + 2H_2O \qquad (2.4)$$

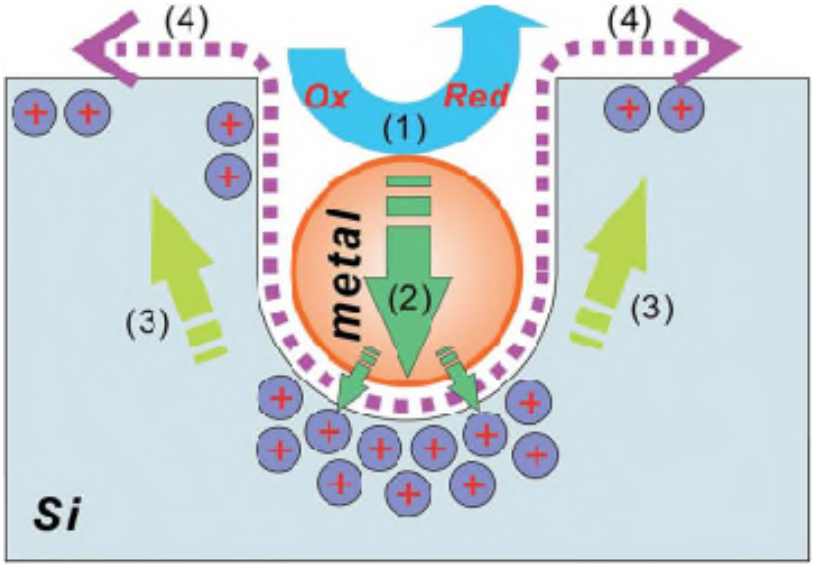


**Figure 3.4** An illustration of the metal-assisted chemical etch process [3].

Figure 3.4 illustrates the metal- assisted chemical etch process which takes place in the following steps:

- The reduction of an oxidative Agent (such as $H_2O_2$) catalyzed by a noble metal particle [29]

- The injection of the holes generated during the reduction reaction, into the Silicon substrate, with the highest hole concentration underneath the metal particle [2]

- The migration of holes to Silicon sidewalls and surfaces [3]

- The removal of oxidized Silicon via HF [4]

Now this system composes of the corrosion-type redox reaction. This comprises of the cathodic reduction of the Ag+ ions and anodic oxidation of the Silicon beneath the deposited Ag.

Then reduction of Ag+ is accelerated chemically since Ag easily attracts electrons from the Silicon substrate, this result in the growth of the Ag nuclei [60, 67]. Also oxidation of Silicon beneath Ag particles to $SiO_2$ occurs which is then dissolved by HF so that holes appear the upper Silicon surface as Ag particles sink [29]. As the reaction goes further Ag particles begin to grow into silver dendrites as their density reaches its saturation point. And when Silicon beneath the Ag particles is etched away to a certain depth, silver nano pillar structures start to appear [29].

This mechanism can be more accurately understood by Figure 3.5 which includes the reaction process (a through g) to formation of nano pillars and can be explained further by the following points (Here, reaction with Au has been explained to depict the use of both Ag and Au in parts, respectively):

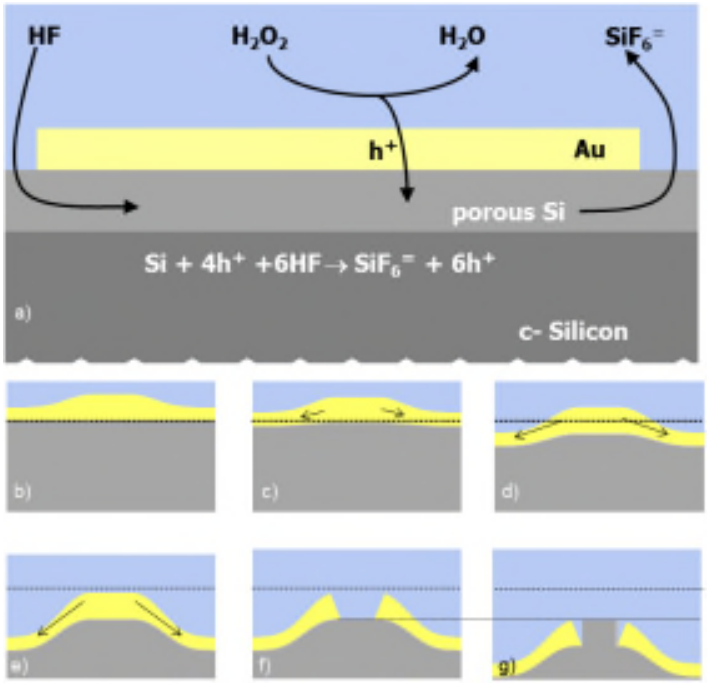


**Figure 3.5** Mechanism of maskless nano pillar formation [23].

- Reduction of $H_2O_2$ at the gold–solution interface injects holes into gold that causes Silicon oxidation at the buried gold–Silicon interface [23]. This mechanism competes with the direct oxidation of Silicon by $H_2O_2$ diffusing through the porous Silicon layer that however dominates only in proximity of the gold pad borders. In both cases, oxidized Silicon gets complexed by HF and out diffuses as $SiF_6^{2-}$ [29].

- Panels (b) through (g) report a schematics of the deformation–delamination mechanism, showing how the differential etching rate due to the metal thickness profile (b) leads to the generation of a strain in the metal layer ((c)–(e)) finally inducing metal delamination (f). The Silicon area no longer covered by gold is then etched at a marginal rate resulting (g) in the formation of the nanopillar. The dashed line marks the initial position of the gold–Silicon interface [23].

**Electrochemical Etching**

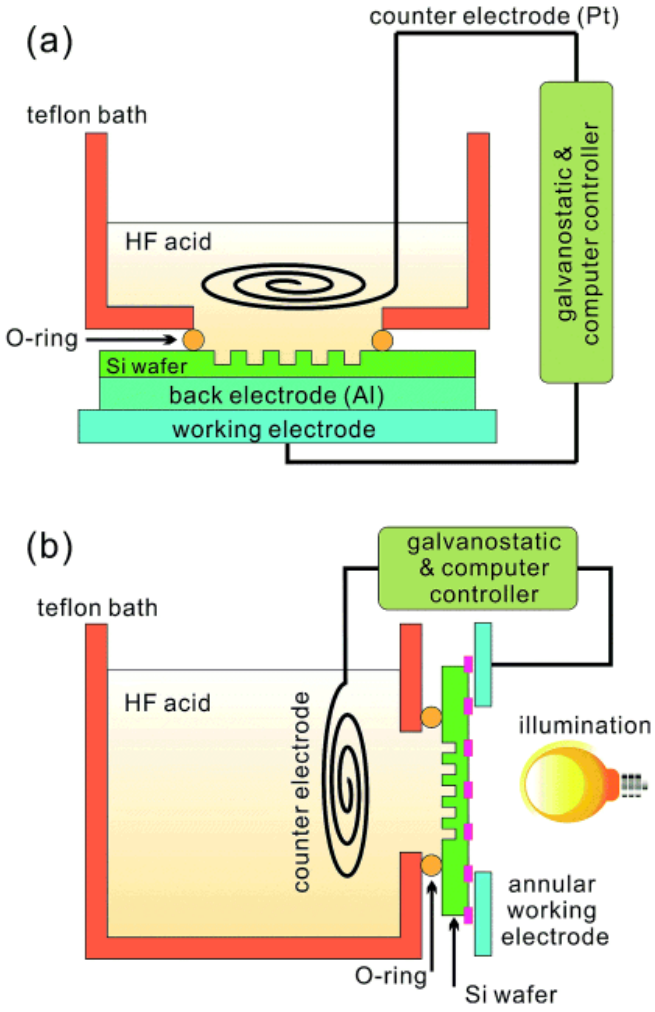


**Figure 3.6** Typical experimental setups for electrochemical HF etching Of: (a) p-Si; And (b) n-Si [3].

This etching popularized mainly after the discovery of luminescence from porous Silicon [3]. This method involves a Silicon wafer which is tied to the anode of an electrochemical cell which is already dipped into a solution which contains HF, water and ethanol [3, 4]. The experimental setups for p-Si and n-Si can be seen in Figure 3.6. Each of which has its separate role.

1. HF: Responsible for removing Silicon oxide by forming a water soluble complex and oxide was produced during the etching reaction [50]

2. $H_20$: Participation in the oxidation reaction and also can control HF's aqueous concentration as well the corresponding reaction rate [50]

3. Ethanol: Improves wettability, allowing the release of HF during the reaction and also the infiltration of HF into the Silicon pores, also reduces surface tension [50]

Then, focusing towards the mechanism of the reaction, etching process is initialized by applying a voltage bias or a current. Based on the current density, the mechanism can take part in 3 regions namely low, high and transition current density regions [3, 4].

- Low current density region: formation of porous Silicon since etching reaction is limited by Silicon dioxide. [5]

- High current density region: High numbers of holes are put into the bulk material and diffuse over the entire region/ surface of the wafer. Also here the reaction is limited by removal of the oxide and the wafer becomes electrochemically polished. [4]

- Transition region: this regain exists in between the other two regions where without using a mask randomly distributed pillars can be formed. [4]

Now, the factors on which the exact current density values which define the 3 regions depend are:

1. Doping type 2. Concentration of the wafer 3. illumination conditions

The main focus is only in the low current density region in case of black Silicon. In the region, etching is mainly controlled by changing the etching time, illumination and current density [17]. The resultant Silicon pore sizes mainly change with current density. Its morphology depends upon wafer doping type and dopant concentration. But the 2 basic methods employed to control the parameters are etching time and current density [7]. The porosity of a Silicon wafer remains and the pores grow by applying a constant current. Also that change in current density can result in the formation of the structures whose refractive indices and porosities vary [5]. The resulting structure reduces the light reflection unto 5% [4, 60, 67].

### 3.3.3 The Laser Method

Dr. Eric Mazur, professor of physics at Harvard University, and several of his graduate students discovered a remarkable semiconductor material known as "black Silicon." [10] They irradiated Silicon with a femtosecond laser; they placed an ordinary Silicon wafer in a vacuum chamber, then filled it with chalcogen-containing gas, and blasted the Silicon with ultra-short, super-intense laser pulses (Figure 3.7) [3,4].

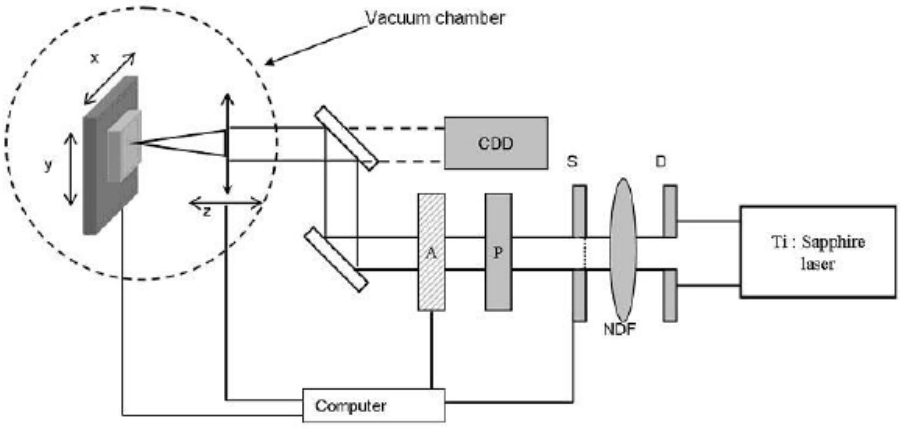


**Figure 3.7** Diagram of the Femtosecond Laser Experimental set-up [9].

The result was a blackened surface covered with a vast array of microscopic spikes that proved to be up to 500 times more sensitive to light than a standard Silicon chip. Although, the first laser- induced cones in Silicon were first studied and seen by Rothenberg and Kelly which can be clearly understood by Figure 3.8 where material around the pit gets eroded after the formation of conical structures [9, 67]. They produced micron-sized conical structures using nano-second UV laser pulses [10]. Experimentally, Single crystal Silicon wafers are cleaned for 10 minutes in 3 different processes one after the other. First, in an ultrasonic trichloroethylene bath this is followed by an ultrasonic acetone bath and then finally ultrasonic methanol bath. These samples are then mounted on a motorized two-axis translation stage inside the vacuum chamber [67]. The gas chamber is pumped out and backfilled with a selected gas. Corrosion resistant MKS capacitance- voltage transducer is used to keep the pressure in check [10].

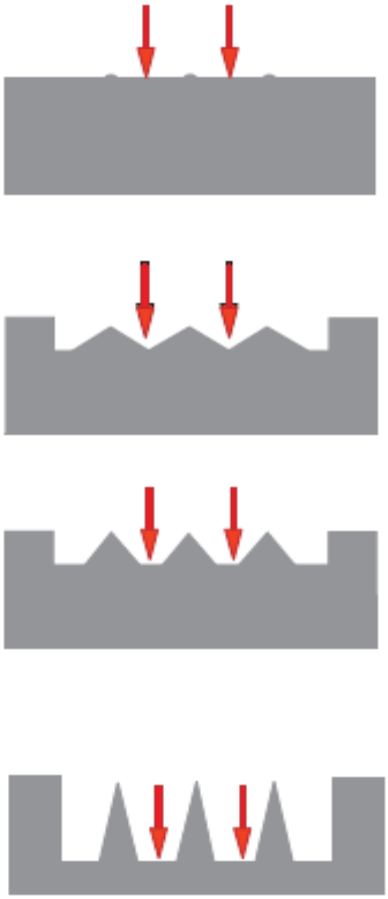

**Figure 3.8** Cone formation in ion sputtering seeded by a protective pit [10].

Ti: sapphire laser system is used to produce 100- femtosecond laser pulses whose wavelength is 800nm at 1 kHz [10]. The pulse rate and pulse duration is changed on the basis of factors like [9]:

- Wave plate-polarizer combination
- Distance of the gratings
- Neutral density filters

The laser beam is then focused and the spot size is measured which usually vary somewhere between 100 and 200 micrometers [9]. Generally white light is used to illuminate the sample [14].

Then, there are two ways in which the wafer is formed based on its structure :

- Method 1: here the sample is exposed to the laser beam to produce spikes over the patches. This is done by adjusting the scanning velocity in reference with the laser bean size [3, 4, 10].

- Method 2: the process of irradiating a single spot on the wafer in the presence of laser beams takes place in this method. Mechanical shutter monitors the number of laser pulses falling on the wafer. Precise hold over the number of laser pulses is also governed in this process. [3, 4, 10].

### 3.3.4 Surface Analysis

### 3.3.1 Science of Surface Roughness

There exist extensively nanostructured surfaces in nature which have lots of unique and amazing functions. Inspired by these functional nanostructures, nano science and nanotechnology are developed and aim to realize similar artificial surfaces with attractive features by micro/nano fabrication techniques [7]. For example:

- Lotus leaf- Promotes self-cleaning ability with a super hydrophobic and low-adhesion surface, due to micro/nano dual-scale structures [7].

- Namibian Desert beetle- Harvests water from tiny water droplets dispersed in the air, because its elytra is covered with a micro/nano structure array of hydrophilic peaks surrounded by hydrophobic background [6].

- Moths- Improve their visual ability by covering their eyes' facets with nanostructures, creating a layer which is almost perfect broadband and anti-reflective [7].

**Table 3.4** Properties of structures used for optical simulation [17]

| Structure | Reflectance (%) | Absorptance (%) |
|---|---|---|
| Spikes | 6 | 94 |
| Penguin- like | 9 | 91 |
| Pillars | 21 | 79 |
| Pyramids | 27 | 73 |
| Flat | 35 | 65 |

All the realizations of the above functions cannot be separated from various nanostructures [15]. The hydrophilic nature and hydrophobicity of nanostructures play important roles in microfluidic systems, while **the anti-reflectivity can be utilized in solar cells, making surface-nanostructured materials attract significant attention** [17]. And those nanostructures with low reflectance are named "black Silicon" due to their

black color to the naked eye. Some nanostructured surfaces have been fabricated by combining anti-reflective surface super hydrophobic surface to offer additional functionalities to photo voltaic or optical sensors for devices with better performance. Among various kinds of nanostructures, including pyramids [17], “penguin like” structures [17], nanopillars [17], nanowires [17] and nanocones [17], it is proved that nanocone/ spiked surfaces are the best structures to lower the reflectance comparison (Table 3.4).

Black Silicon is a material that is chemically equal to normal Silicon [15]. The only difference between these two is the surface treatment that changes the morphology [48, 52]. This special morphology has to represent a certain roughness of the surface and it is typically done by creating pyramid textures or trenches or cones or spikes within the Silicon [4]. When these structures are in place, and when they are small enough, incident light is more absorbed and less reflected [53].

Since five different ways have been elucidated previously in chapter 3 to fabricate black Silicon, below is the comparison between various surfaces on the basis of SEM images obtained by those methods:

**3.3.2 Reactive Ion Etching**: In the SEM image (Figure 3.9), it can be noticed that this etching/passivation competition mechanism leads to the formation of random Silicon microstructures with very high aspect ratios in a self-masking fashion-

- (a) and (b) - Top and side views of BSi, with RF power = 1500 W, bias = 40 V, $O_2/SF_6$ = 0.09, pressure = 10 Pa, time = 10 minutes.

- (c) and (d) - top and side views of BSi, with RF power= 1500 W, bias= 30 V, $O_2/SF_6$ = 0.07,pressure = 3 Pa, time = 30 minutes.

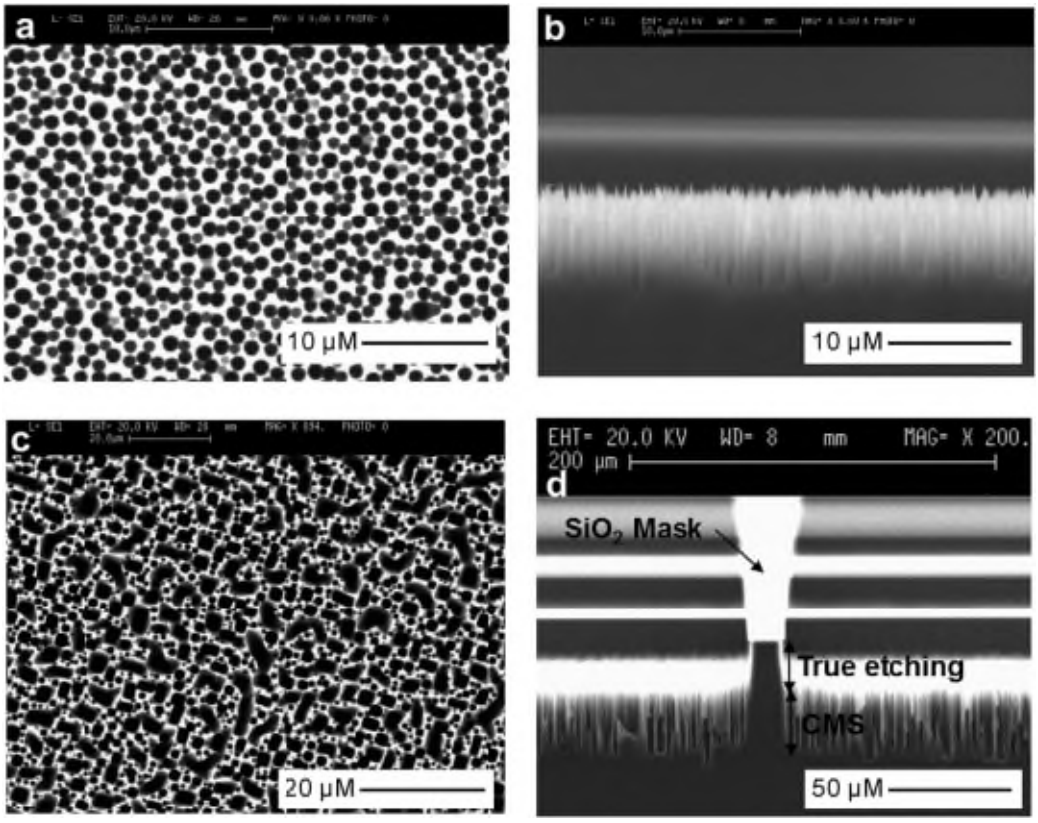


**Figure 3.9** SEM images of BSi fabricated by RIE under different conditions [3].

**3.3.3 Plasma Immersion Ion Implantation**: The images in Figure 3.10 show unique microstructures of the black Silicon. The black Silicon surface exhibits a needle-like structure. The average height of the needle is about 2 micron [1, 3, 4]. The porous or needle like structure of the black Silicon will be formed under the competition of $SF_x^+$ (x ≤ 5) and $F^+$ ions etching effect, $Si_xO_yF_z$ passivation and ion bombardment [59]. The unique microstructure leads to multiple reflections for incoming light.

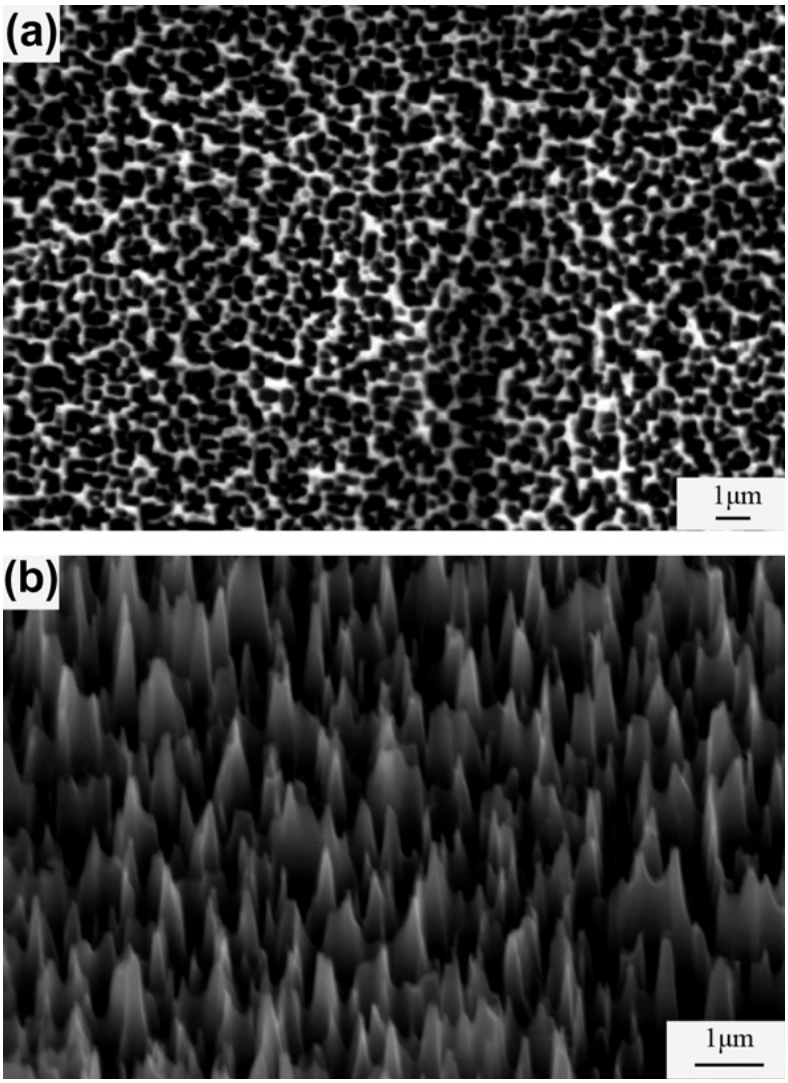


**Figure 3.10** SEM images of unique microstructures of the Black Silicon. (a) Top View, (b) side view (viewed at 30° to the normal) [4].

**3.3.4 Bosch RIE Process**: The structures are formed by this process when $CF_6$ and $C_4F_8$ are alternatively introduced into the reaction chamber for etching and passivation, respectively [3, 4, 57]. And by repeating this process for hundreds or even thousands of cycles, a very deep and near-vertical Silicon needle structure can be fabricated. Figure 3.11 depicts:

1. SEM image of BSi formed by Bosch RIE process

2. SEM image of a single Silicon “needle” produced by Bosch RIE process, with undulated side wall.

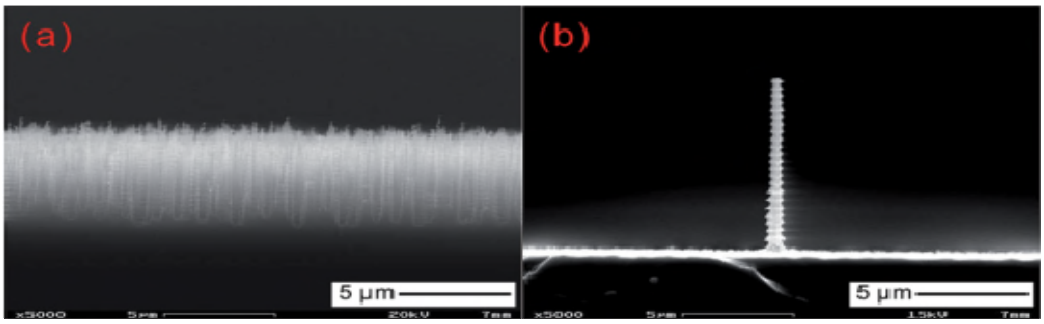


**Figure 3.11** SEM images of needle structured Black Silicon [3].

**3.3.5 Metal Assisted Chemical Etching**: With scanning microscope, it is possible to compare the difference in morphology between the reference sample and those with different structures and layers [2, 54, 51].

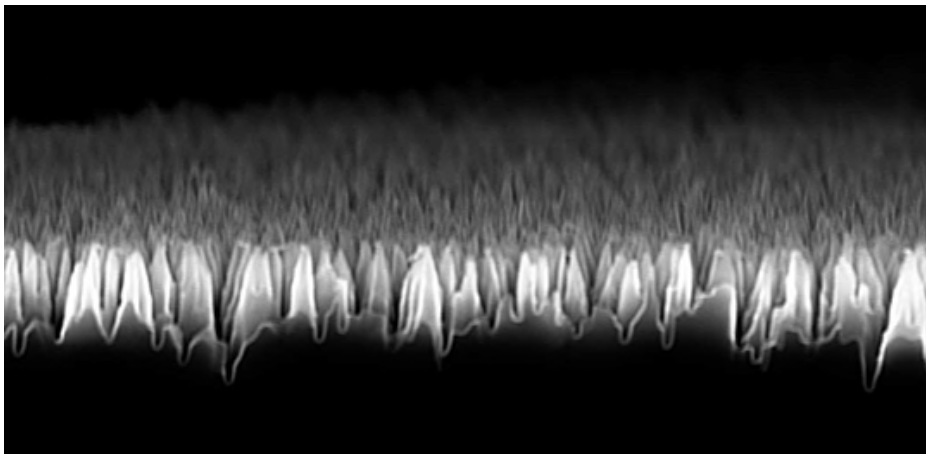

**Figure 3.12** SEM image of a pyramid textured Black Silicon surface [2].

Figure 3.13 Shows SEM images of black Silicon sample where the thickness of the Au metal is 7 nm [2, 29]. The annealing temperature of these samples was 500°C and the annealing time is taken to be 10 minutes. Figure 3.13(a) explains:

- When Au metal is annealed at high temperature, the metal atoms diffuse and make gold particles.
- The temperature of this annealing is made high so as to increase the kinetics of diffusion Au atoms will make Nano-sized particles.
- Clearly spaced gold particles with an average size of 131 nm.

Figure 3.13(b) depicts the same sample but after it was etched with HF and $H_2O_2$ for 120 seconds [2, 60]:

- From this Figure, black dots on the brighter background can be seen.
- These black spots are supposedly the holes where the metal particles sink down.
- This could be further argued by the fact that the average size of these black spots (holes) is 122 nm which is in a good correlation with the average size of the Au particles.
- These two pictures are very critical in explaining the whole process of making the black Silicon.

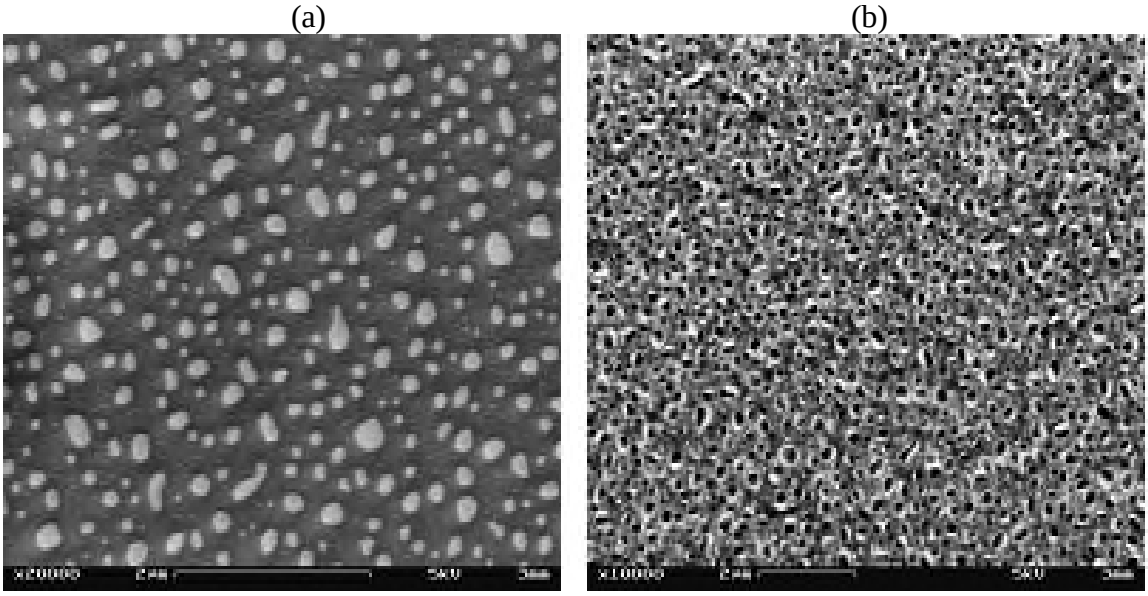


**Figure 3.13** SEM image of sample after annealing (a) and after etching (b) [2].

**3.3.6 Femtosecond Laser Method:** Formation of sharp, micron-sized spikes were observed after a Silicon surface was irradiated with hundreds of femtosecond laser pulses in the presence of $SF_6$ or $Cl_2$. The spikes exhibit a sharp tip with a subtended angle of less than 20°. The spikes characteristics depend on laser and gas conditions. They can be several tens of microns tall and the tip-to-tip separation is several microns. The spikes form gradually over hundreds of laser pulses. The series of SEM pictures in Figures below show how the spikes develop successively as the number of laser pulses increases using 100-femtosecond laser pulses of 10 kJ/$m^2$ fluence. The sample was irradiated in 500 torr of $SF_6$.

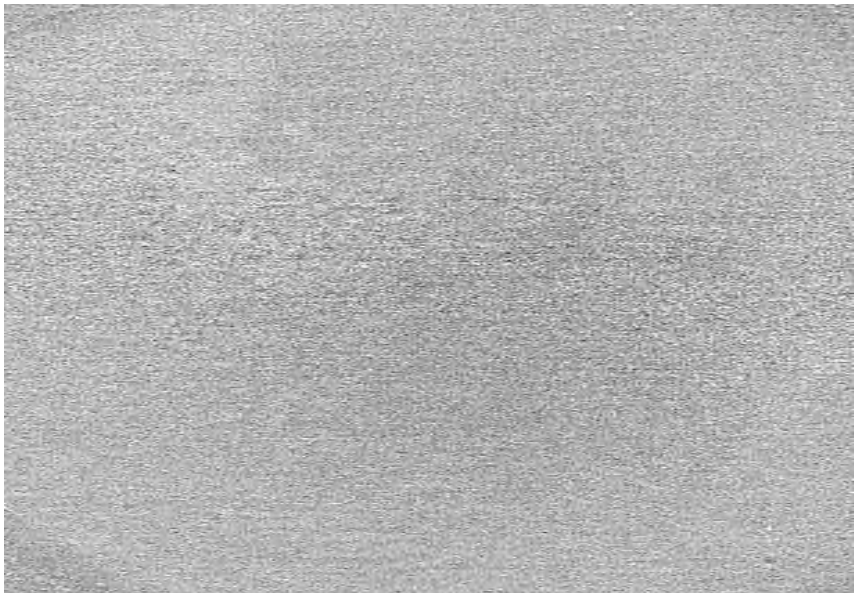

**Figure 3.14** Silicon surface after 0 pulses. After a single laser pulse, point-like defects are observed [10].

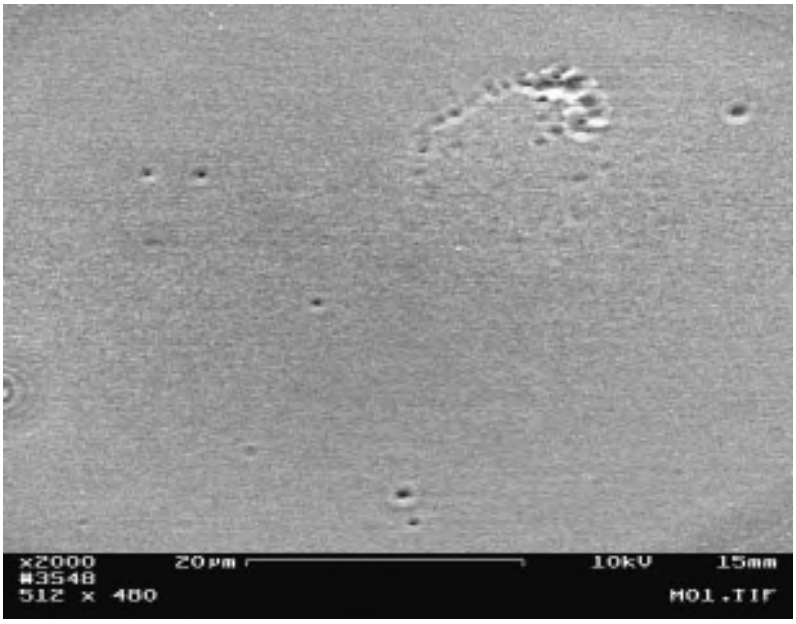


**Figure 3.15** Silicon surface after 1 pulse [10].

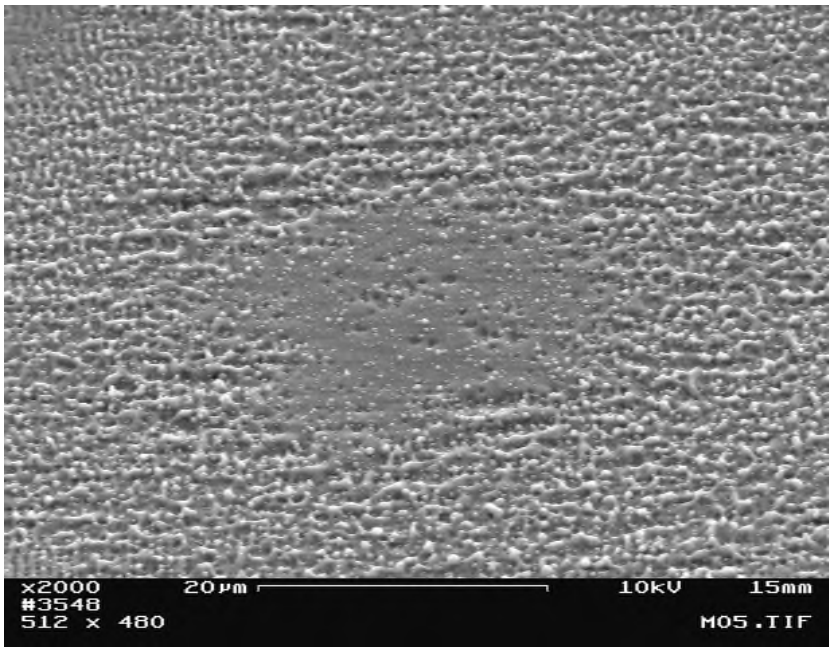


**Figure 3.16** Silicon surface after 5 pulses. After 5 pulses a grain-like structure emerges [10].

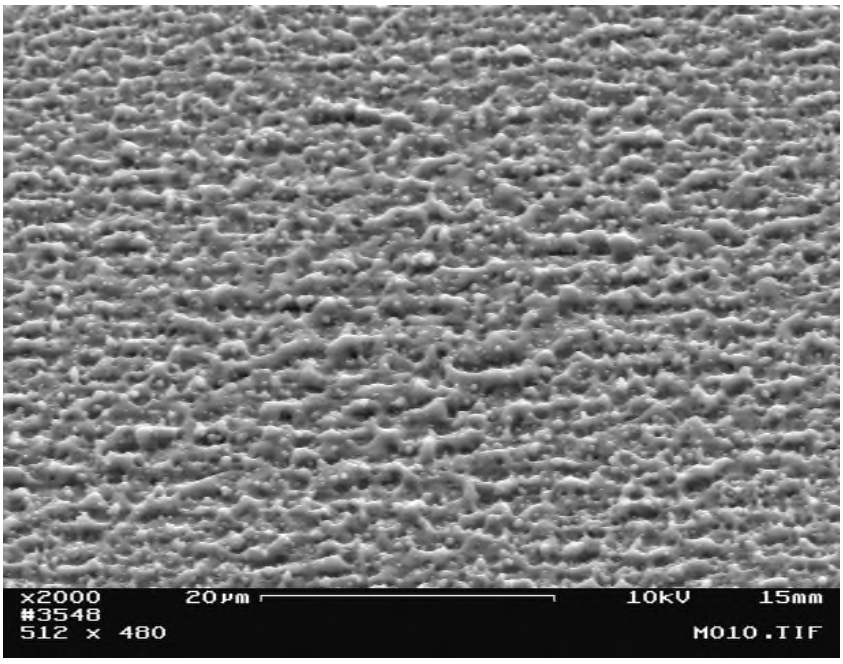


**Figure 3.17** Silicon surface after 10 pulses. After 10 pulses rippled structure is observed [10].

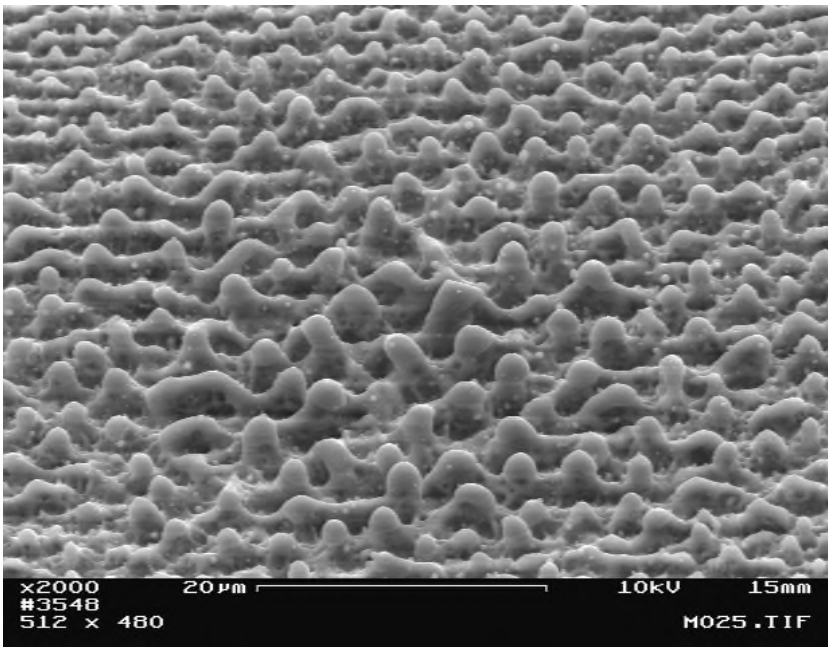


**Figure 3.18** Silicon surface after 25 pulses. Forms segregated protrusions after 25 pulses [10].

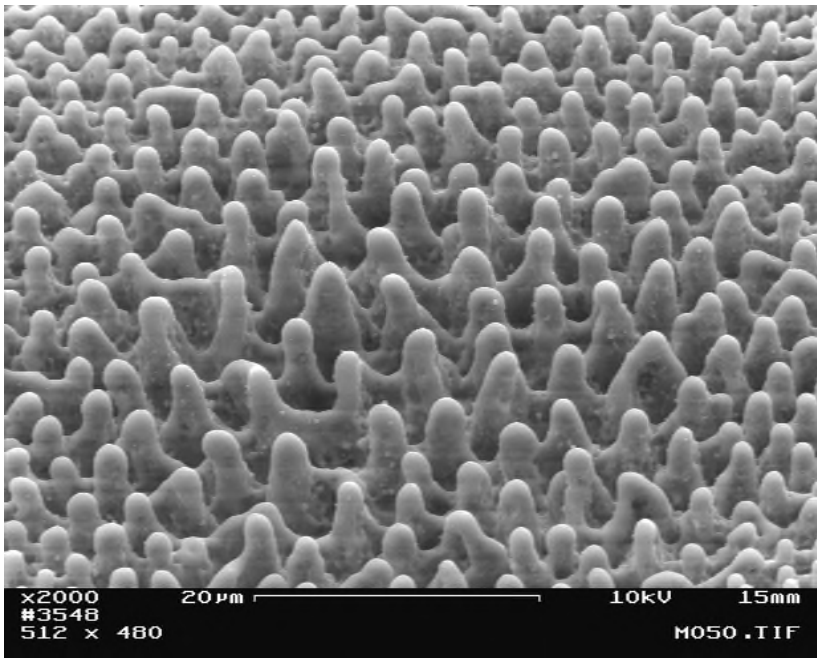


**Figure 3.19** Silicon surface after 50 pulses. At this point the final distribution of spikes is determined. The protrusions develop into sharp spikes after several hundred laser pulses in the following images [10].

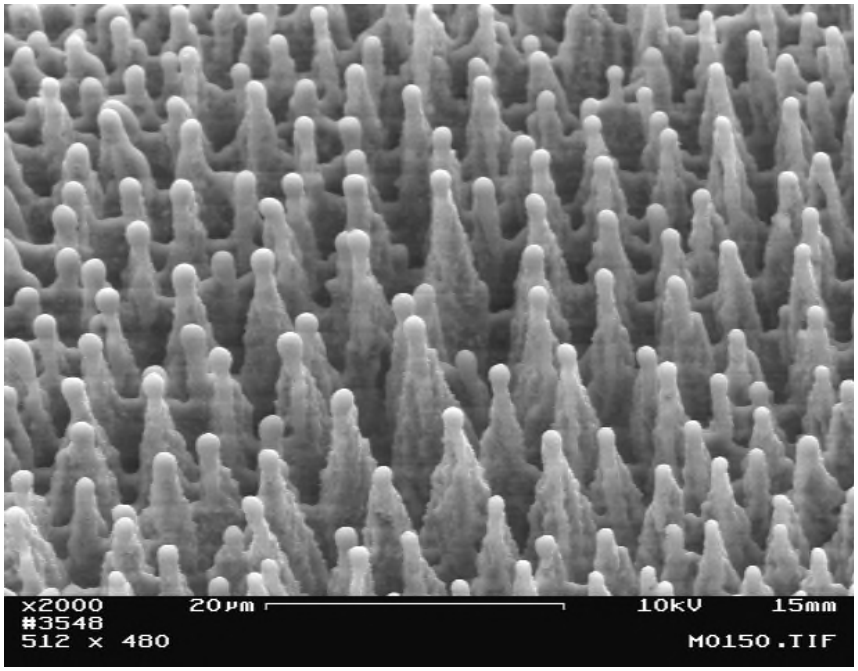


**Figure 3.20** Silicon surface after 150 pulses [10].

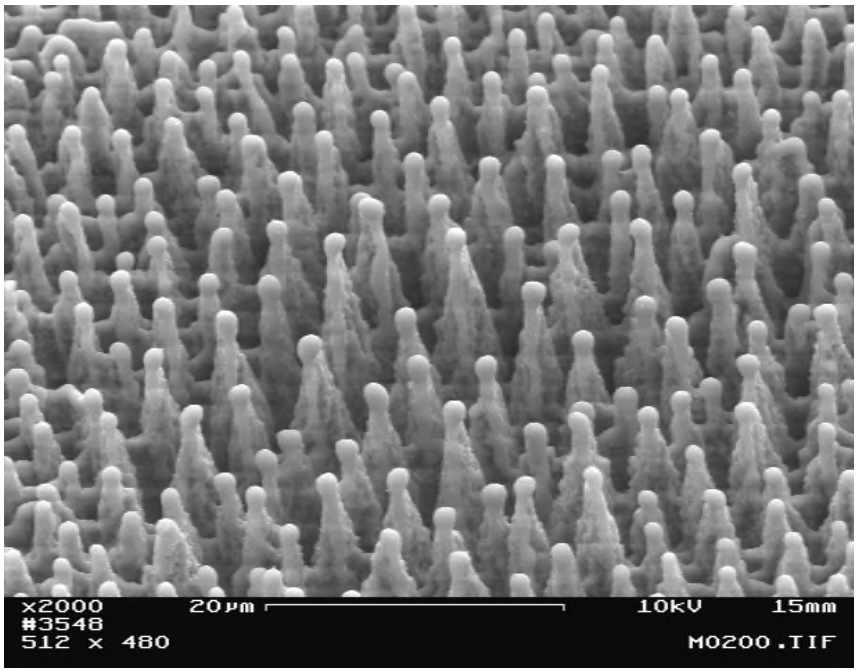


**Figure 3.21** Silicon surface after 300 pulses [10].

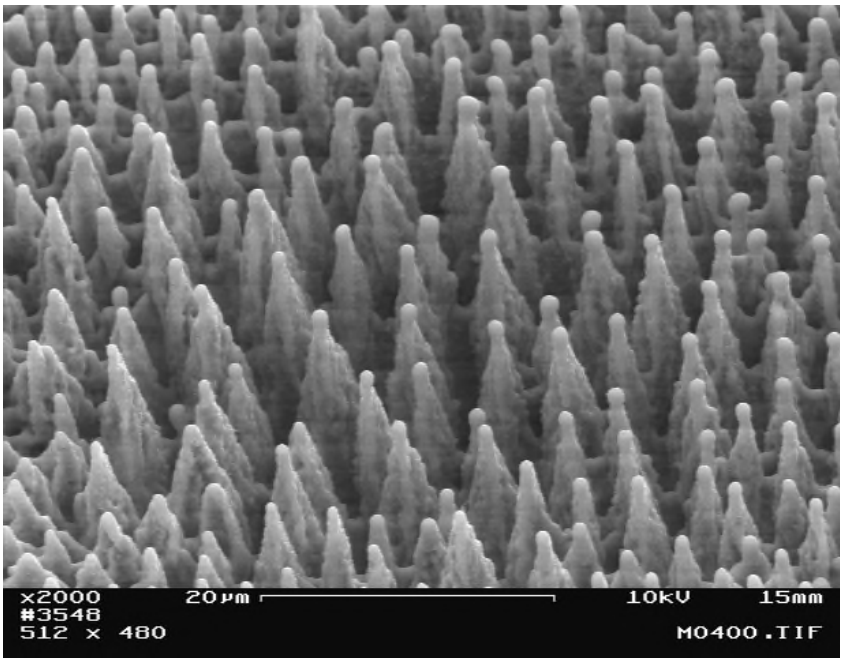


**Figure 3.22** Silicon surface after 450 pulses [10].

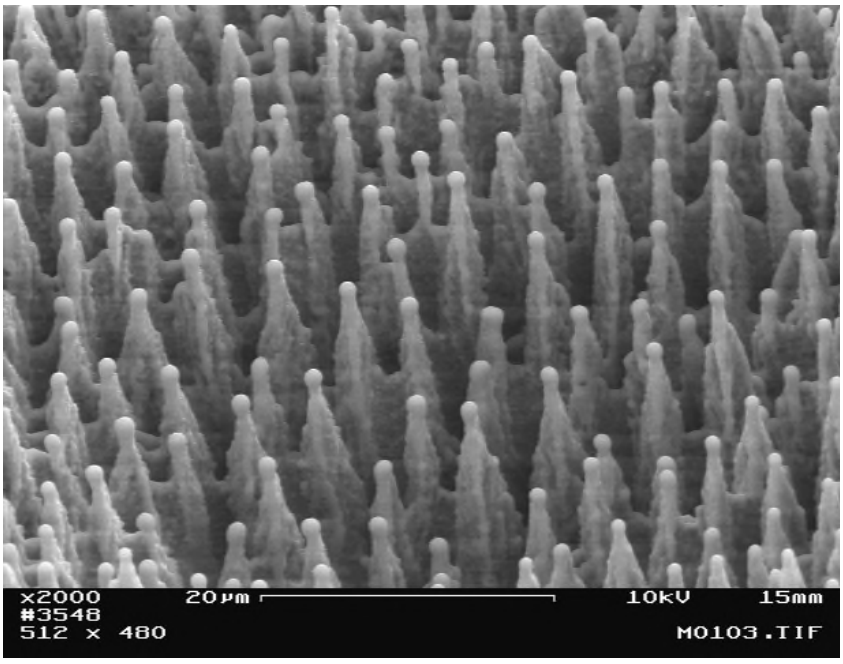


**Figure 3.23** Silicon surface after 1000 pulses. The spikes become thinner until after a few thousand laser shots the spikes are destroyed and a crater is left behind. [10]

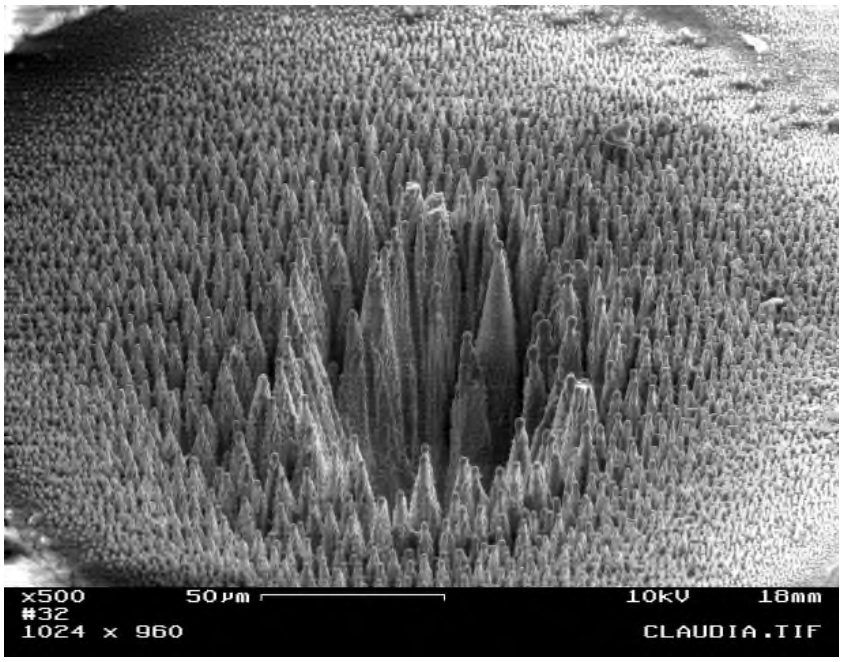


**Figure 3.24** Silicon surface after 1500 pulses. A crater is visible in the center, the remaining spikes are thinned. A cutaway view of the spiked surface is formed [10].

The presence and the nature of the gas are crucial to spike formation. Sharp spikes were only formed in $SF_6$ and $Cl_2$. Structures form in vacuum, nitrogen, helium, or argon, but they are blunt and irregular. Given below is the Figure 3.25 which depicts the comparison between structures formed in presence of $SF_6$ and in vacuum.

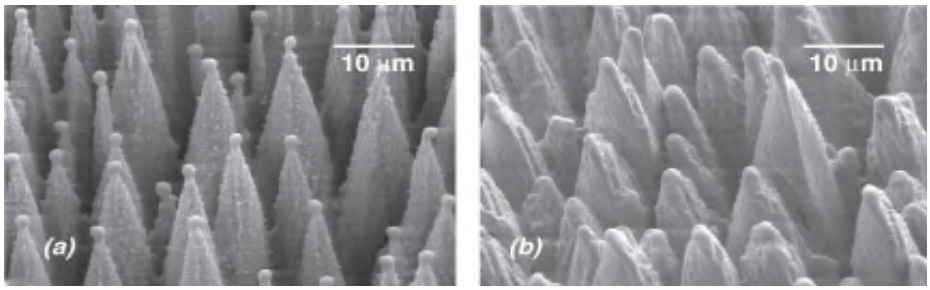


**Figure 3.25** Comparison of structures formed in (a) $SF_6$ and (b) vacuum as seen under the SEM at a 45° view [10].

### 3.3.7 Comparison of the Surfaces by Methods Discussed

The basic comparison between the morphologies of black Silicon formed by different techniques is given below:

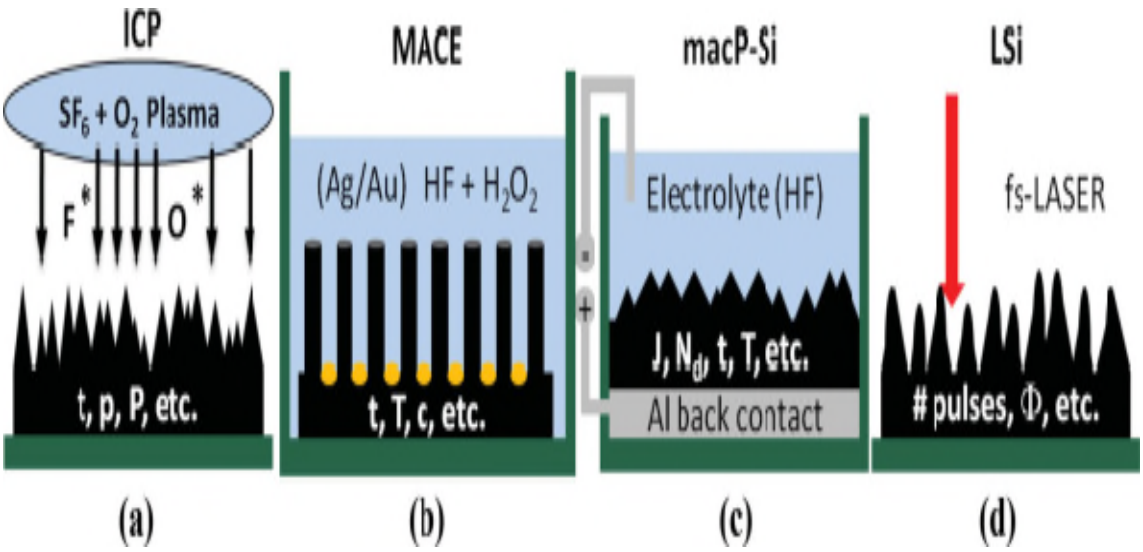


**Figure 3.26** Schematic diagrams of the four used fabrication methods (not at scale) [15].

The Figure 3.26 summarizes the shape and form by following ways:

a) Shows the inductive coupled plasma reactive ion etching (ICPRIE, or short ICP) process in an atmosphere of $SF_6$ and $O_2$

b) Depicts the metal assisted wet chemical etching (MACE) process based on Ag or Au catalyst particles in aqueous solutions of HF and $H_2O_2$

c) Shows the electrochemical etch cell used for macro-porous Silicon (macP-Si) fabrication

d) Depicts the experimental setup for the fs-laser-treated Si surfaces

From Figure 3.26, and chapter 3 leads to a final comparative study on the basis of fabrication methods (table 3.3).

**Table 3.5** Comparative study of methods and properties [4]

| Synthetic Method | Reagents | Catalyst | Structure Of BSi | Cost | Reflectance (%) | Shortcomings(If Any) |
|---|---|---|---|---|---|---|
| **RIE** | $SF_6/O_2$, $SF_6/Cl_2/O_2$, $SF_6/O_2/CH_4$ | None | Pyramid to needle-like | High | 4 | High Energy Consumption Or Complicated Fabricating Processes |
| **PIII** | $SF_6/O_2$ | None | Needle-like | High | 1.79 | Extreme Sensitivity To Many Variables Like Pressure, Power, And Flow |
| **MACE** | $AgNO_3$ /HNO/HF | Au, Ag | Column to needle-like | Low ( Solution based metal catalyst) | 0.3 | Diffusivity Of Noble Metal Catalysts In Si Is Slow |
| **ELECTRO-CHEMICAL** | HF, $H_2O$ | None | Mountain shaped | Low | <5 | Needs External Current And Electrodes, Inconvenient For Mass Production |
| **LASER** | $CCl_4$, $C_2Cl_3F_3$, $SF_6$, $Cl_2$, $N_2$, | None | Spiked | High | 2.5 | Inefficient For Large Area BSi Texturing |

## CHAPTER 4

## OPTICAL PROPERTIES

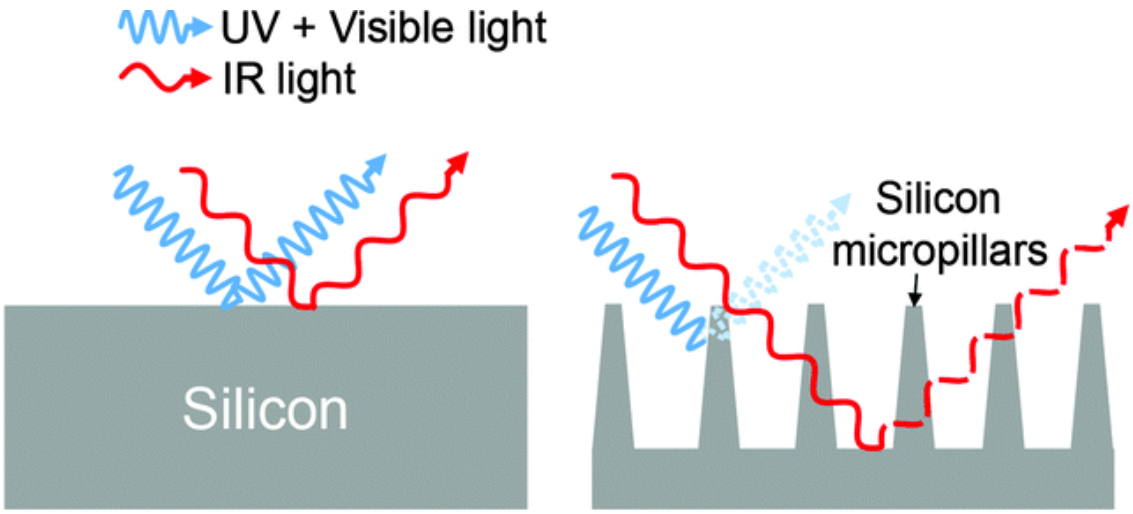


**Figure 4.1** Schematic diagram of reflection from a polished silicon surface showing strong reflection of UV, Visible And IR Light in comparison with silicon micro pillars which strongly absorb not only UV+Visible light but also IR light [24].

"Optical property" refers to a material's response to exposure to electromagnetic radiation and, in particular, to visible light. It is basically the property which is a function of its interaction with EM radiation whose wavelengths lie in visible region (0.4-0.7 microns) spectrum [24]. And this concept primarily applies to black Silicon mainly since black Silicon is capable of absorbing all incident light i.e. from near- UV to mid- IR. This property chiefly makes black Silicon have an edge over to normal Silicon which can partly absorb any radiation and photon energies below band gap (1.11 eV which corresponds to 1.1 microns) are transmitted through it. Also, the absorption properties

of microstuctured Silicon are not affected by the band gap photon energies [3, 4, 24]. In fact, due to additional anti-reflection properties of black Silicon, the absorption reaches near unity with energies greater than band gap [7, 8].

We are aware that when light proceeds from one medium into another (e.g., from air into a solid substance), 3 basic actions, might take place:

- Some of the light radiation may be transmitted through the medium
- Some will be absorbed, and
- Some will be reflected at the interface between the two media.

The above mentioned properties are inter-related by a given formula:

$$\mathbf{A(\lambda) + R(\lambda) + T(\lambda) = 1} \qquad (4.1)$$

Where: A (λ) – Absorptance, R (λ) – Reflectance, T (λ) – Transmittance

## 4.1 Comparison of Black Silicon Optical properties Formed With Various Fabrication Methods

### 4.1.1 RIE- PIII

Figure 4.2 and 4.3 shows the reflectance values for black Silicon formed by RIE and PIII respectively. In case of RIE, reflectance is observed to be as low as 1.05% which is a lot lower than crystalline Silicon's reflectance which can be as high as 50% [8, 42, 48].

Similarly, in the case of PIEEE average reflectance of the black Silicon can be reduced to 1.79% over the wavelength ranging from 300 nm to 1100 nm [1, 59].

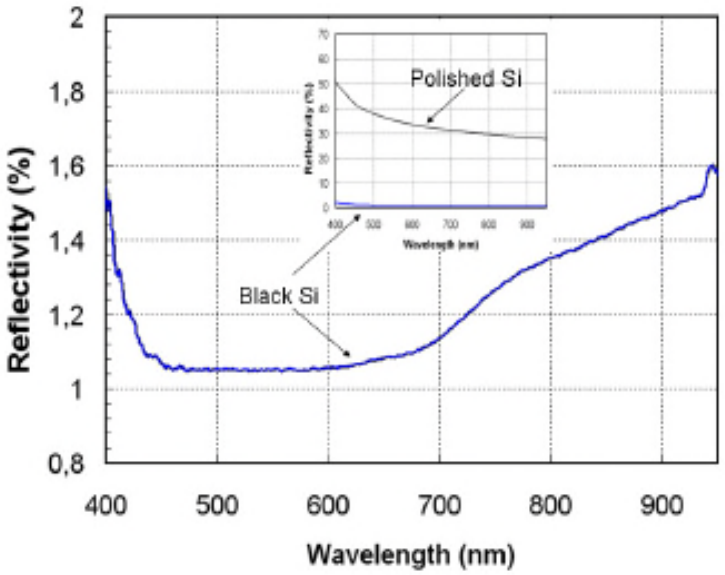


**Figure 4.2** Measured Reflectance Spectra Of Black Silicon Under Normal Incidence [8].

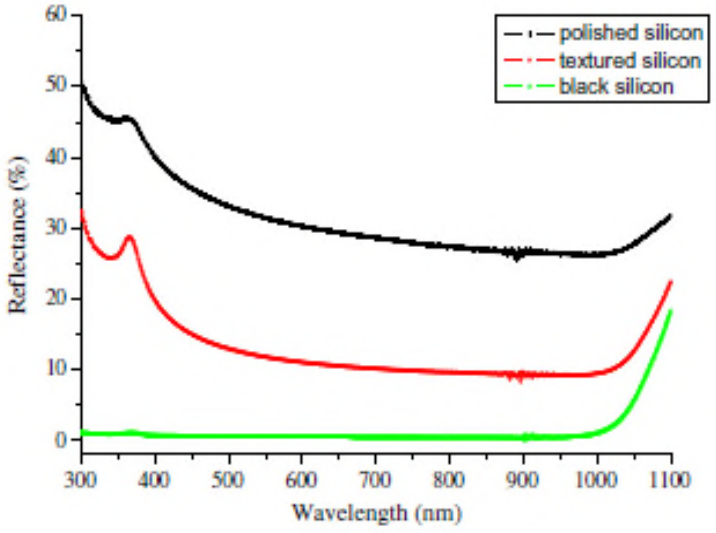


**Figure 4.3** The Reflectance Of Polished, Textured And Black Silicon [1].

### 4.1.2 Metal Assisted Etching

In Figure 4.4 during the process, Au nano particles have been fabricated via thermal annealing of Au thin films with 1, 3 and 7 nm thickness [2]. It was found that the initial Au film thickness could affect the particle size and change the etching conditions and improve optical properties of the surface. The absorption significantly increased and the reflection decreased drastically in the wavelength range from 250 to 1100 nm [2, 54]. Similar experiment performed with Ag (Figure 4.5) depict the average reflectivity of the resulting black Silicon in the wavelength range from 300 nm to 1100 nm to be 8.2%, while that of conventionally acid textured Silicon is 28.6% [2, 3, 4]. However, the reflectivity of black Silicon increased more rapidly than conventionally acid textured Silicon above 1100 nm (Figure 4.5). This phenomenon is mainly credited to the increased band gap and the enhanced backward-scattering caused by nanopillars [29].

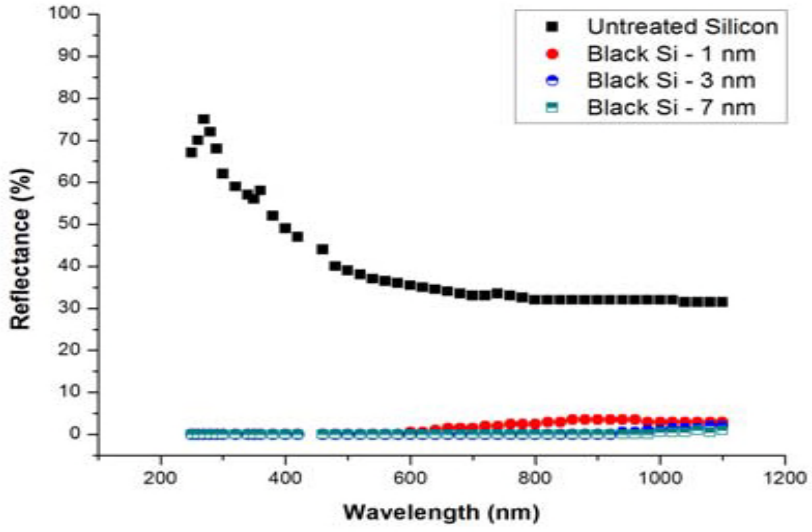


**Figure 4.4** Normal Incidence Spectral Reflectance From Black Si Surface Etched With Various Au Film Thicknesses (1, 3 And 7 Nm) And From Untreated Silicon Surface [2].

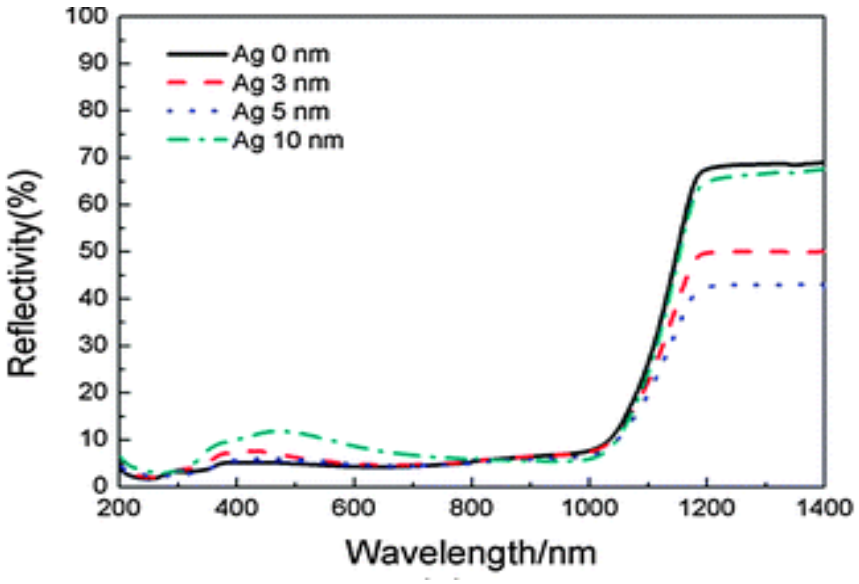


**Figure 4.5** Total Hemispherical Reflectance Of Black Si Covered With A 30 Nm $Sin_x$ Layer And 0 Nm, 3 Nm, 5 Nm, 10 Nm Mass Thickness Of Ag [29].

### 4.1.3 The Laser Method

Figure 4.6 shows the measured reflectance of the three spiked surfaces and the flat, untreated surface. The taller the spikes, the less the reflectance and transmittance (and consequently the greater the absorptance, by equation 4.1, 5.1, 5.2) [59, 16, 17]. The absorptance is greater than 0.9 for 500 nm- 2500 nm for the sample with 10-12 µm spikes and reflectance reduces to 0.1 when compared to crystalline Silicon [62, 66]. However, the biggest change in the optical properties occurs on going from ordinary Silicon to the sample with spikes only 1-2 µm tall [3, 4].

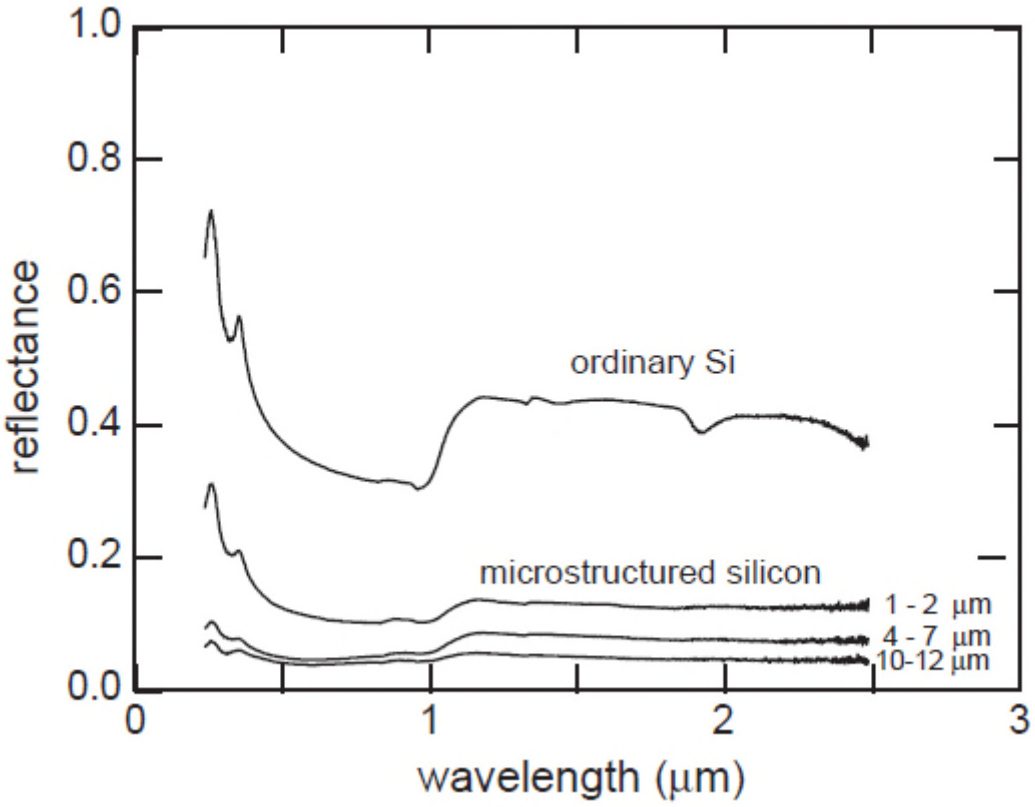


**Figure 4.6** Reflectance Of The Three Spiked Surfaces And Ordinary Silicon [10].

### 4.1.4 Light Trapping Technique

Since, already optical reflectance has been established and compared for black Silicon formed by all technique's discussed in chapter 3 and because black Silicon possesses few unique properties from bulk Silicon, anti-reflection and improved absorptance makes it the most fitting candidate for solar cell components leading to its major contributions to light trapping [24]. Anti-reflective (AR) coatings are thin films applied to surfaces to reduce their reflectivity through optical interference. An AR coating typically consists of a carefully constructed stack of thin layers with different refractive indices

[24]. The internal reflections of these layers interfere with each other leading to an overall reflectance lower than that of the bare substrate surface [3, 4, 25].

Below (Figure 4.7 and Figure 4.8) is a schematic comparison between how anti-reflection coating and black Silicon surface differs and absorbs and traps all the incoming light:

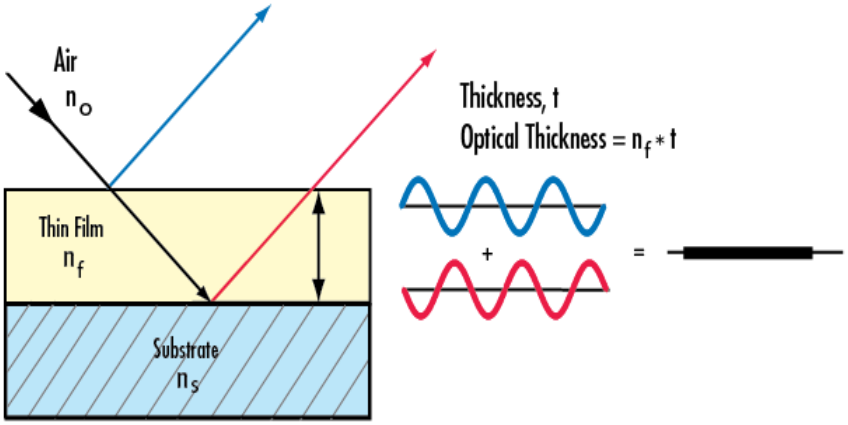


**Figure 4.7** Illustration of light interacting with thin film [25].

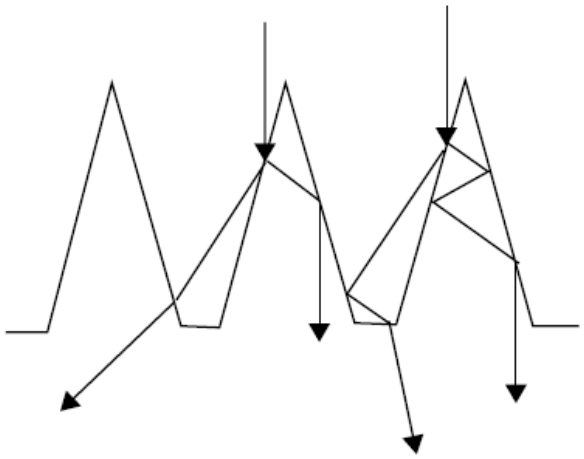

**Figure 4.8** Schematic showing light trapping through multiple reflections [10].

The comparison clearly proves how inner as well as the outer surface micro structure can capture maximum radiation through multiple reflections. A significant reduction in reflectance to a few percent in the visible and to about 20% 3 in the infrared has been analyzed [25]. Whereas in Figure 4.7, The transmission properties of a coating are dependent upon the wavelength of light being used, the substrate's index of refraction ($n_s$), the index of refraction of the coating($n_f$), the thickness of the coating(t), and the angle of the incident light [3, 25]. This is basically the main disadvantage, since they are not capable of trapping radiations of all wavelengths.

From graph 4.9 it can be observed that, as light passes through an uncoated glass substrate, approximately 4% is reflected at each interface. This results in a total transmission of only 92% of the incident light.

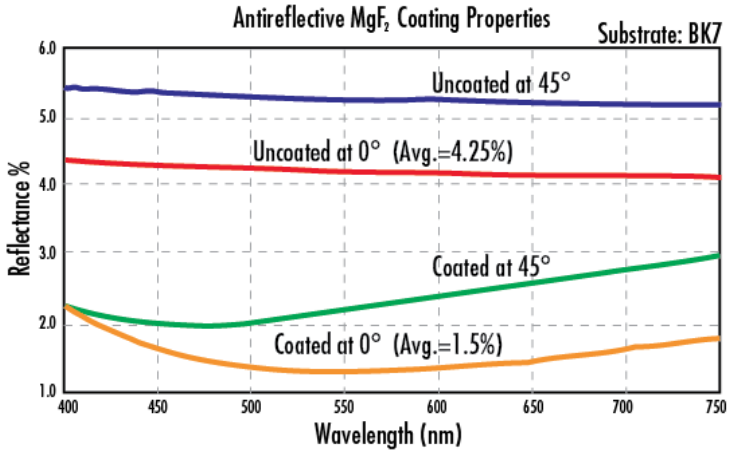


**Figure 4.9** General anti-reflection coating performance [25].

Whereas in comparison to BSi, in Figure 4.10 given below, it can be clearly noted that the lowest reflectance is way below 4% [24, 25]. Since, the surface majorly depends upon the etching time, the graph shows variation of reflectance with wavelength at

different etch times [26]. Curves shown in the Figure also demonstrate the effect of increasing pore depth on the reflectance of the longer (i.e., near band edge) wavelength light incident on the surface.

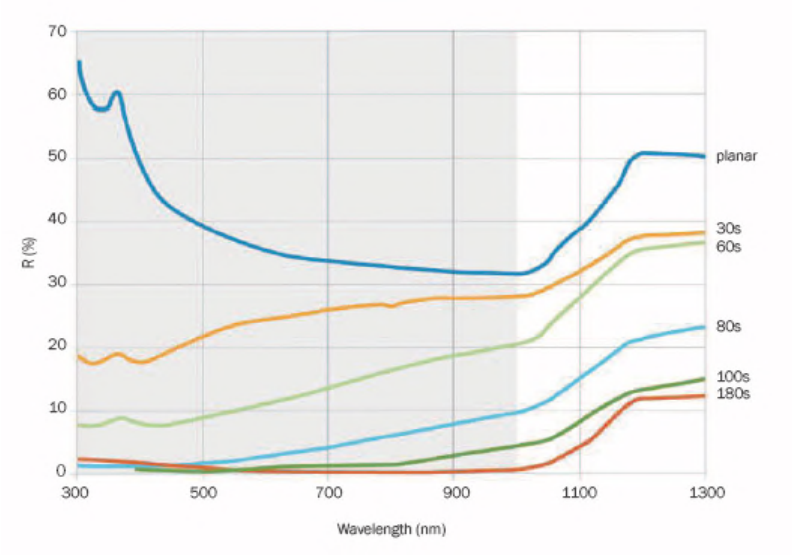


**Figure 4.10** reflectance from black silicon surface [26].

Table 4.1 elucidates various other light trapping methods used in the industry with their shortcomings and then a detailed comparison of different types of solar cells and black Silicon solar cells have been analyzed. These other anti- reflections are being used in present time and the listed shortcomings have been overcome by black Silicon according to the analysis. Black Silicon proves to be a better resort to any other light trapping method.

**Table 4.1** Shortcomings of Various Anti-Reflection Techniques used in Industry

| Method | Shortcomings |
|---|---|
| **Amorphous Silicon** | Major Application in solar panels but these panels have a lower efficiency due to the disordered nature of amorphous Silicon; solar cells are subject to the Staebler-Wronski effect [13], which reduces the solar cell efficiency by up to 15 percent. Tiny voids within the Silicon network are partly responsible for reducing solar cell efficiency and those micro voids most likely contribute to light-induced degradation of amorphous Silicon thin film solar cells. |
| **Carbon Nano-tubes(CNTs)** | Combining carbon nanotubes (CNTs), graphene or conducting polymers with conventional Silicon wafers leads to promising solar cell architectures with rapidly improved power conversion efficiency. Problem is that efficiency of polymer solar cells is only limited to a few percent and also there are issues in the donor-acceptor material of polymer. The inherent problem of conducting polymer seems to be the main constraint [27]. |

| | |
|---|---|
| **Transparent Conductive Oxide (TCO) Films** | Indium tin oxide is one of the most widely used transparent conducting oxides because of its two chief properties, its electrical and optical transparency. The main concern about the high cost and limited supply of Indium and its fragility and lack of flexibility of ITO layers [61]. The fragility is mainly due to mechanical pressure caused by small vibrations in the films. By minimizing the Absorption losses, stable efficiencies of only about 15% seems to be achievable [28]. |
| **Cadmium Sulphide, Cadmium Telluride** | High cost of rare metals, lack of reliable and precise deposition techniques. There are health concerns with the use of cadmium in thin-film solar cells. Cadmium is a highly toxic substance that, like mercury, can accumulate in food chains. This is a blemish on any technology that fancies itself part of the green revolution [13, 30]. |

**Table 4.2** Shortcomings of Various Anti-Reflection Techniques Used in Industry (Continued)

Contents in table 4.2 have been combined together and presented in a form of comparative study which clearly defines how black Silicon solar cells have an edge over other competitors in the Industry.

**Table 4.3** Comparative Study of Crystalline, Amorphous and Black Silicon Solar Cells [56, 63, 68, 70, 75]

| Factors | Crystalline Solar Cells | Amorphous Solar Cells | Black Silicon Solar Cells |
|---|---|---|---|
| Advantages | Crystalline Silicon (C-Si) solar cells are currently the most common solar cells in use mainly because C-Si is stable, due to the ease of fabrication, and highly reliable. | Available in thin wafer sheets, they are more flexible and easier to handle. They're also less susceptible to damage than their Silicon rivals. | Only up to a micron thick, reflectance is reduced to as low as 0.3% and absorbs 90% incoming light. |
| Efficiency | Delivers efficiencies in the range of 15% to 25% | Less efficient, delivers efficiency in the realm of 20% to 30% of light-to-voltage conversion. | Delivers 18.2% efficiency and don't need extra anti-reflection layers. |
| Absorptance | C-Si is a poor absorber of light and, what might be a sin in this micro-miniature Age, it needs to be fairly thick and rigid. | Suffer significant degradation in power output when they're exposed to the sun. Thinner a-Si cells overcome this problem, but thinner layers also absorb sunlight less efficiently. | Excellent absorber of light, absorbs all incoming light in visible and infrared region |
| Types | Two types of C-Si are in common use: monocrystalline and multicrystalline. Cut from a high-purity single crystal, monocrystalline Silicon consists of 150-mm diameter wafers measuring 200 mm thick. | Typical thin-film solar cells are one of four types depending on the material used: amorphous Silicon (a-Si) and thin-film Silicon; cadmium telluride (CdTe); copper indium gallium deselenide (CIS or CIGS); and dye-sensitized solar cell (DSC). | No types have been discovered until now. |

| | | | |
|---|---|---|---|
| Cost | Even in the form of scrap, crystalline Silicon wafers are not exactly inexpensive based on the efficiency levels they achieve. | Has the potential to be significantly less expensive and at least comparable in efficiency and reliability | Cost effective, since they don't need any anti-reflection coatings. |
| Structure | A basic C-Si cell consists of essentially seven layers | Thin-film solar cells consist of about six layers | Surface modification of Silicon leads to formation needle-like structures that trap enough light. |
| Applications | Even though, they have a low absorption coefficient and are rigid and fairly fragile, they represent about 90% of the world total PV cell production. | These qualities make a-Si cells great for smaller-scale applications, such as calculators, but less than ideal for larger-scale applications, such as solar-powered buildings. | NREL estimates that the black Silicon can reduce processing costs by 4 to 8 percent, resulting in overall savings in manufacturing a solar cell of 1 to 3 percent. Also used in photovoltaics, sensors, anti-bacterial activities. |

**Table 4.4** Comparative Study of Crystalline, Amorphous and Black Silicon Solar Cells

**Table 4.5** Study of Solar Cells With Respect to Efficiency, Thickness and Cost [70, 75]

| Solar Cell Technology | Max Lab Efficiency | Typical Cell Thickness | Si Use | Cost |
|---|---|---|---|---|
| **Mono-crystalline Silicon (C-Si)** | **27.6%** | **~200µm** | **High** | **$$$** |
| **Poly-crystalline Silicon (p-Si)** | **20.4%** | **~200µm** | **Moderate** | **$$** |
| **Amorphous Silicon Thin Film (a-Si)** | **12.5%** | **<1µm** | **Low** | **$** |

# CHAPTER 5

## RESULTS

The main motive of the thesis was to obtain a semiconductor material by the most feasible way possible and compare its optical properties to prove that this material is the best choice possible to attain maximum absorptance (A) and least reflectance which would make it the mist suitable candidate for the solar industry having an edge over all the other anti-reflection techniques already existing in the market.

A good solar cell must satisfy two important conditions. The first is that the active, light-absorbing, material in the cells must be "optically thick" so that every incoming photon can be used to generate electrons and holes. However, the material must not be too physically thick or these photo generated carriers will recombine before they have time to be extracted and produce useful current [74, 75]. One way to satisfy both of these criteria is to use relatively pure (and therefore expensive) materials as the absorbing layer, an option that solar cells manufacturers are not too keen on. However, there may be another way: increasing the amount of light absorbed by a thin layer of conventional photovoltaic material by using light-trapping techniques [62].

And to everyone’s surprise, Black Silicon has been able to satisfy all the important conditions that make it the most potential candidate in Solar Industry. Silicon Black successfully proves to a promising entrant to the world of Solar Energy. The proof that makes it so promising is depicted in Figure 5.1. As targeted, the absorptance values escalated and reflectance values dropped after calculations and simulation.

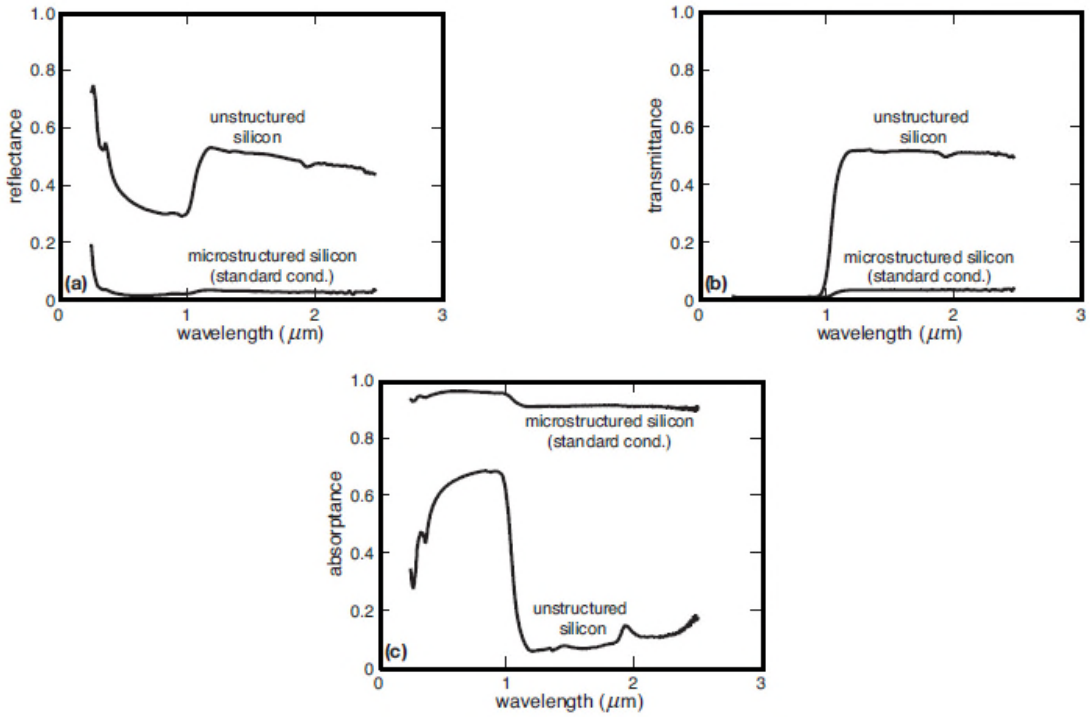


**Figure 5.1** (a) Reflectance (b) Transmittance and (c) Absorptance Of BSi. For Reference, Similar Measurements Are Shown For C-Si in This Figure [10].

Since BSi is just a surface modification of Si, rather than being a material itself, it is difficult to define precise optical constants. Optical constants are not constant in BSi, but rather they will depend on the morphology of the material. By utilizing the effective medium approximation approach, we have defined an effective refractive index and an effective extinction coefficient based on phenomenological approaches.

Under conditions of normal incidence, Reflectance (R) and Transmittance (T) are given by:

$$R = ((n_1 - n_2)^2 + k^2)/ ((n_1 + n_2)^2 + k^2) \quad (5.1)$$

$$T = e^{-\alpha t} \quad (5.2)$$

Where:

Absorption coefficient is the measure of absorption which is given by $\alpha = 4\pi k/\lambda$, $n_1$ and $n_2$ are the refractive indices and k is the extinction coefficient.

R, T, α, A, n and k are function of wavelength, λ. Since B-Si is insensitive to the angle of incidence, we can consider normal incidence for all purposes of calculation. The medium 2 here is air, $n_2 = 1$. The effective n and k are calculated from the R, T and A values obtained from Figure 5.1 and by using equations.

The calculated effective refractive indices and extinction coefficients are plotted below:

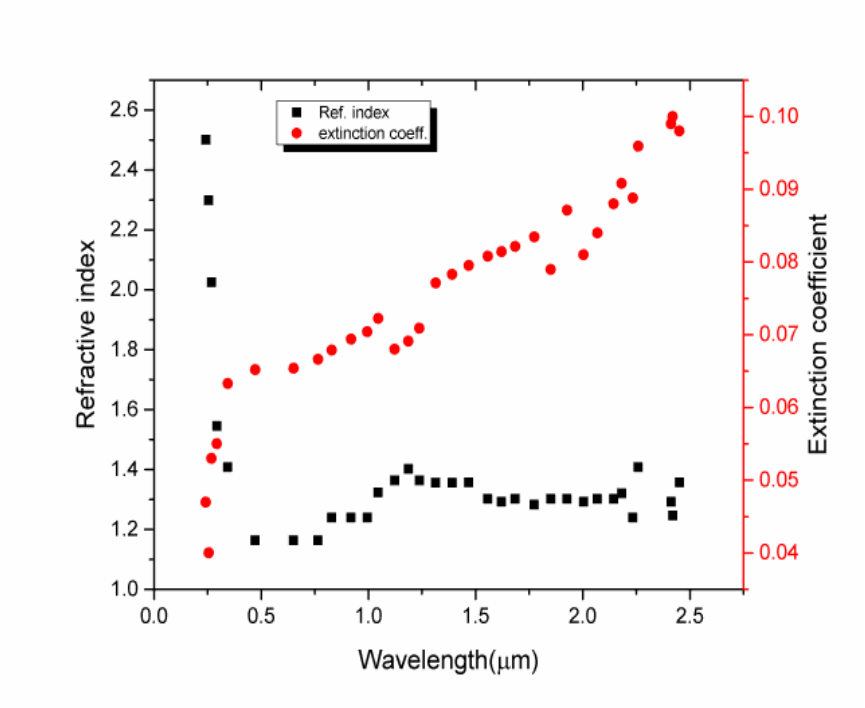


**Figure 5.2** Refractive Index And Extinction Coefficient As A Function Of Wavelength For BSi [81].

From Figure 5.2, a sudden change in both refractive index and extinction coefficient can be observed around the wavelength of 1.1 µm – 1.2 µm [81]. This wavelength region corresponds to the energy gap.

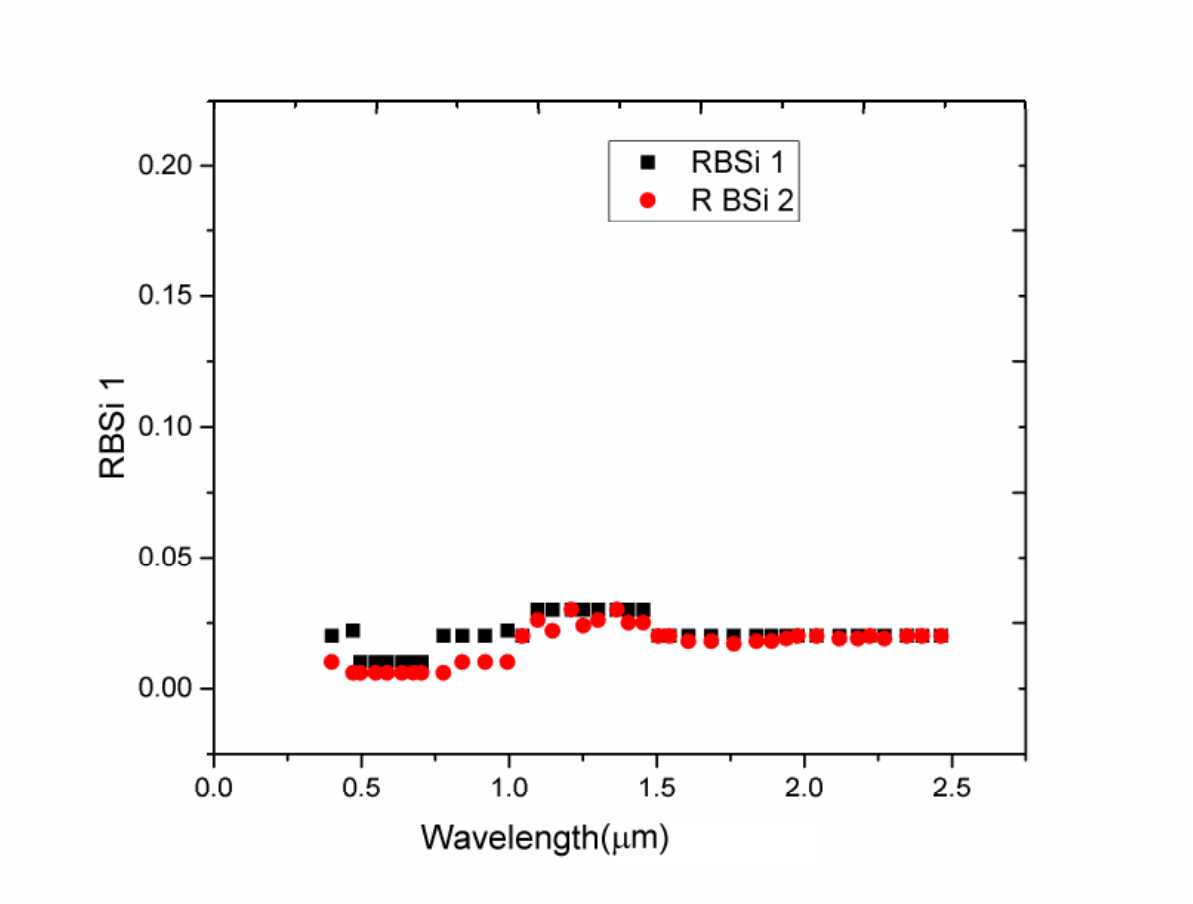


**Figure 5.3** Comparison Of Reflectance, Experimentally Obtained, For BSi *(R BSi1) And Simulated Reflectance For BSi, Based On Effective Refractive Indices And Extinction Coefficients (R BSi2) [81].

*The R for experimental BSi is taken from Figure 5.1

From Figure 5.3, it can be noted that the experimental and simulated values of reflectance of B-Si are generally in accord with each other. Differences in the simulated

and experimental values of reflectance of B-Si are due to the discrepancies in refractive indices and extinction coefficients of C-Si considered in the simulations of the optical properties of the multilayer model (B-Si/C-Si).

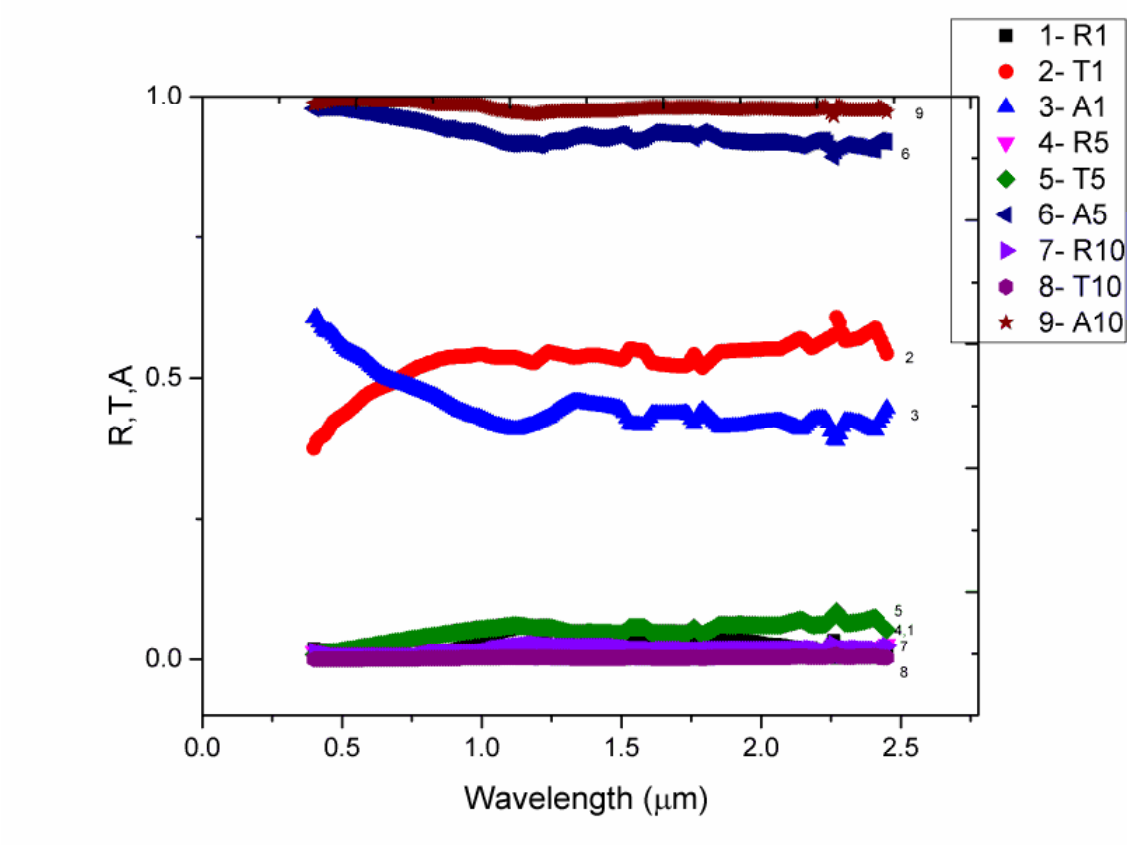


**Figure 5.4** Simulated R, T, A Of BSi Of Different Thicknesses (1 μm, 5 μm And 10 μm, As Function Of Wavelength) [81].

It can be observed from Figure 5.4 that the absorptance of BSi increases significantly with increase in thickness. It can be correlated with the etching time in Figure 4.4. As the time of etching increases in the metal assisted chemical etching process, R decreases. Similarly, R decreases with increasing thickness. T also follows a similar pattern and is evident from Figure 5.4. The dependence of R, T and A on

wavelength for different thicknesses of B-Si can be seen in Figures 5.5, 5.6 and 5.7 respectively.

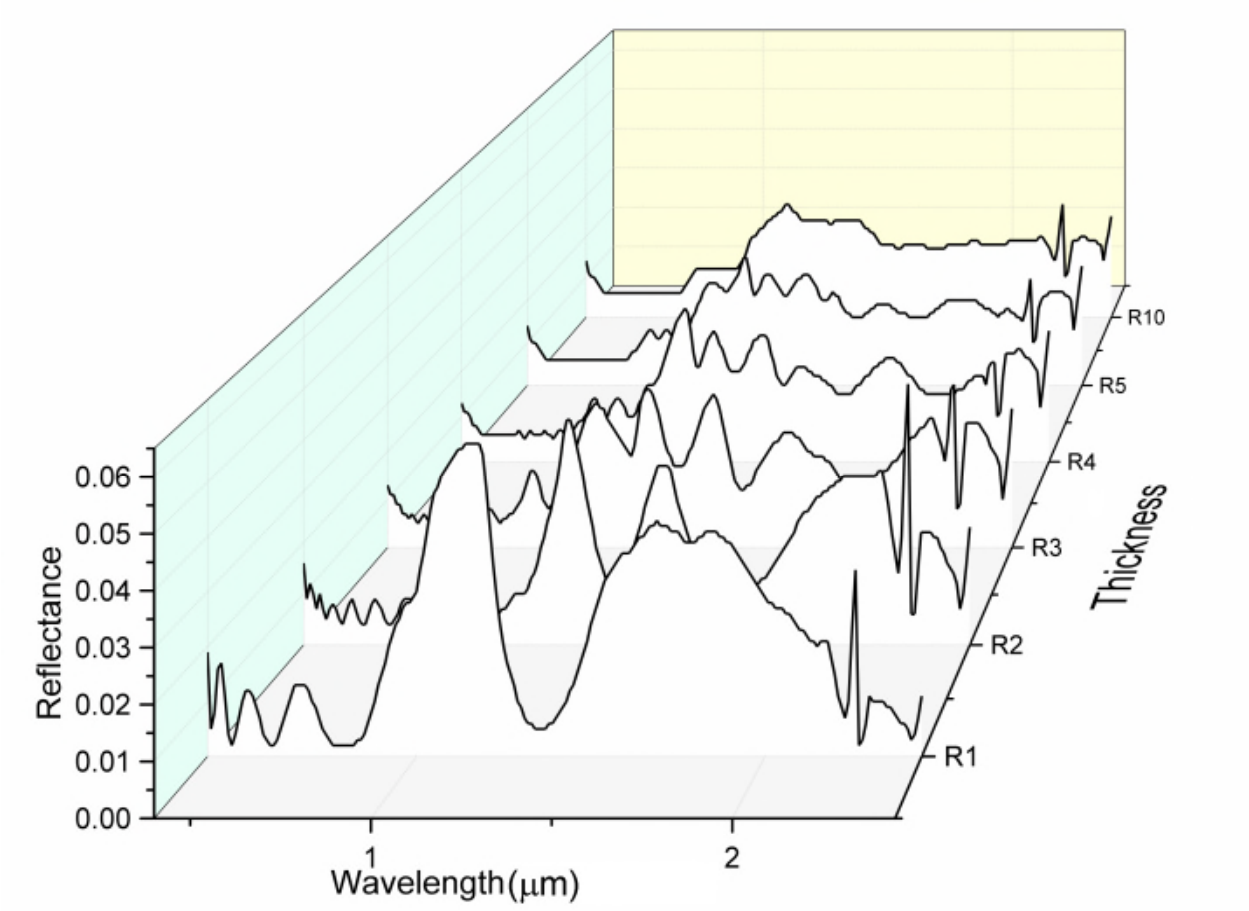


**Figure 5.5** Reflectance of bsi of different thicknesses of B-Si: R1 - 1 μm, R2- 2 μm, R3 - 3 μm, R4 – 4 μm, R5 - 5 μm, R10 – 10 μm, as a function of wavelength [81].

In Figure 5.5, the peak in reflectance for black Silicon, around 1.1 μm, corresponds to the band-gap energy of crystalline Silicon (1.07 eV). Black Silicon has a drastically decreased reflectance and Transmittance almost over the entire measured spectrum. Low Transmittance and low reflectance results in near unity absorptance in

the entire wavelength region. The reflectance in the IR region also decreases as the thickness of BSi increases. This is the result of “blackness” of BSi.

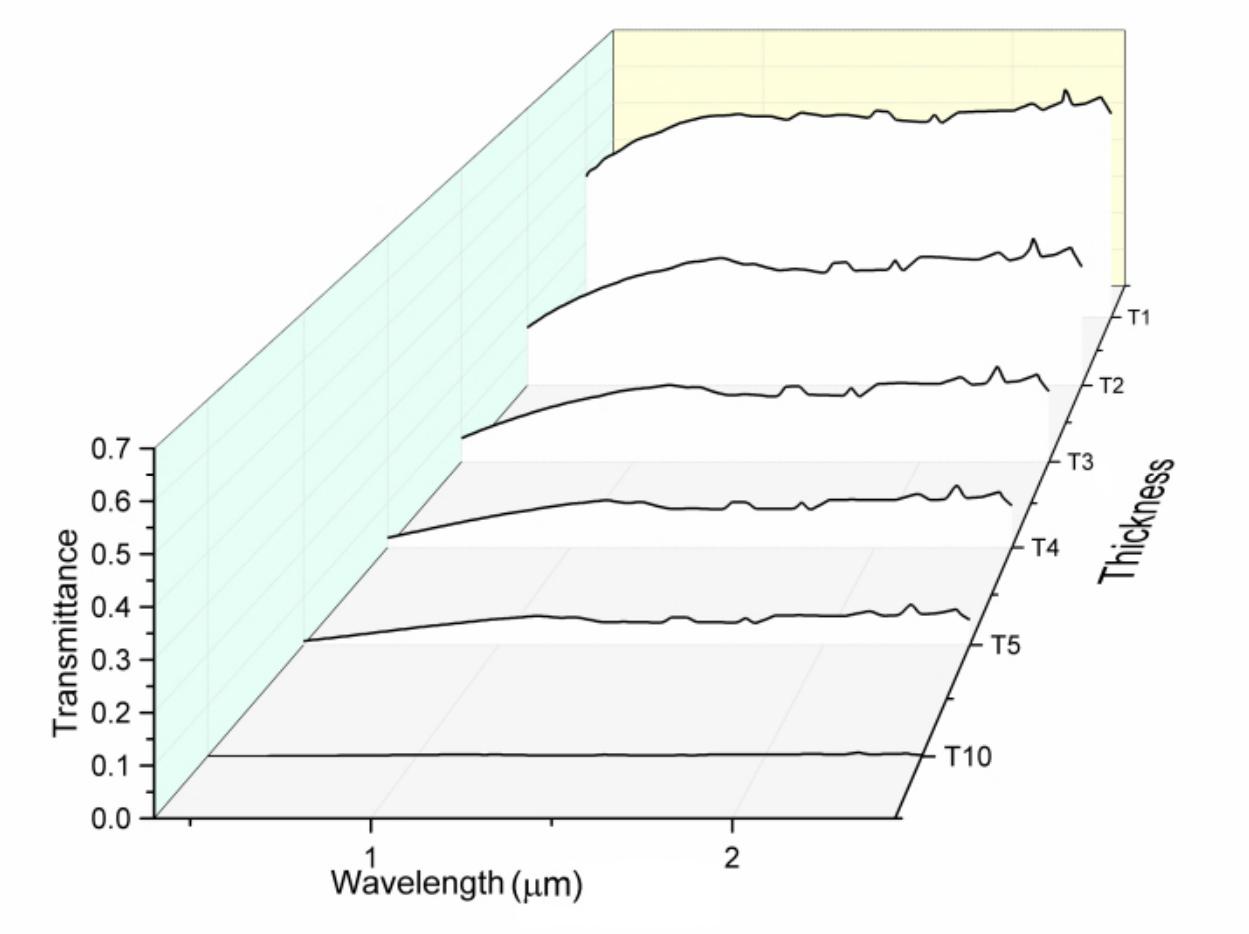


**Figure 5.6** Transmittance of BSi Of different thicknesses of B-Si: T1 - 1 μm, T2 - 2 μm, T3 - 3 μm, T4 – 4 μm, T5 – 5 μm, T10 – 10 μm as a function of wavelength [81].

From Figure 5.6, it can be observed that the Transmittance of B-Si decreases as a function of increasing thickness of B-Si. It is almost zero for 10 μm thick BSi. The Transmittance of BSi, with 1 μm thickness, is almost same as that for C-Si.

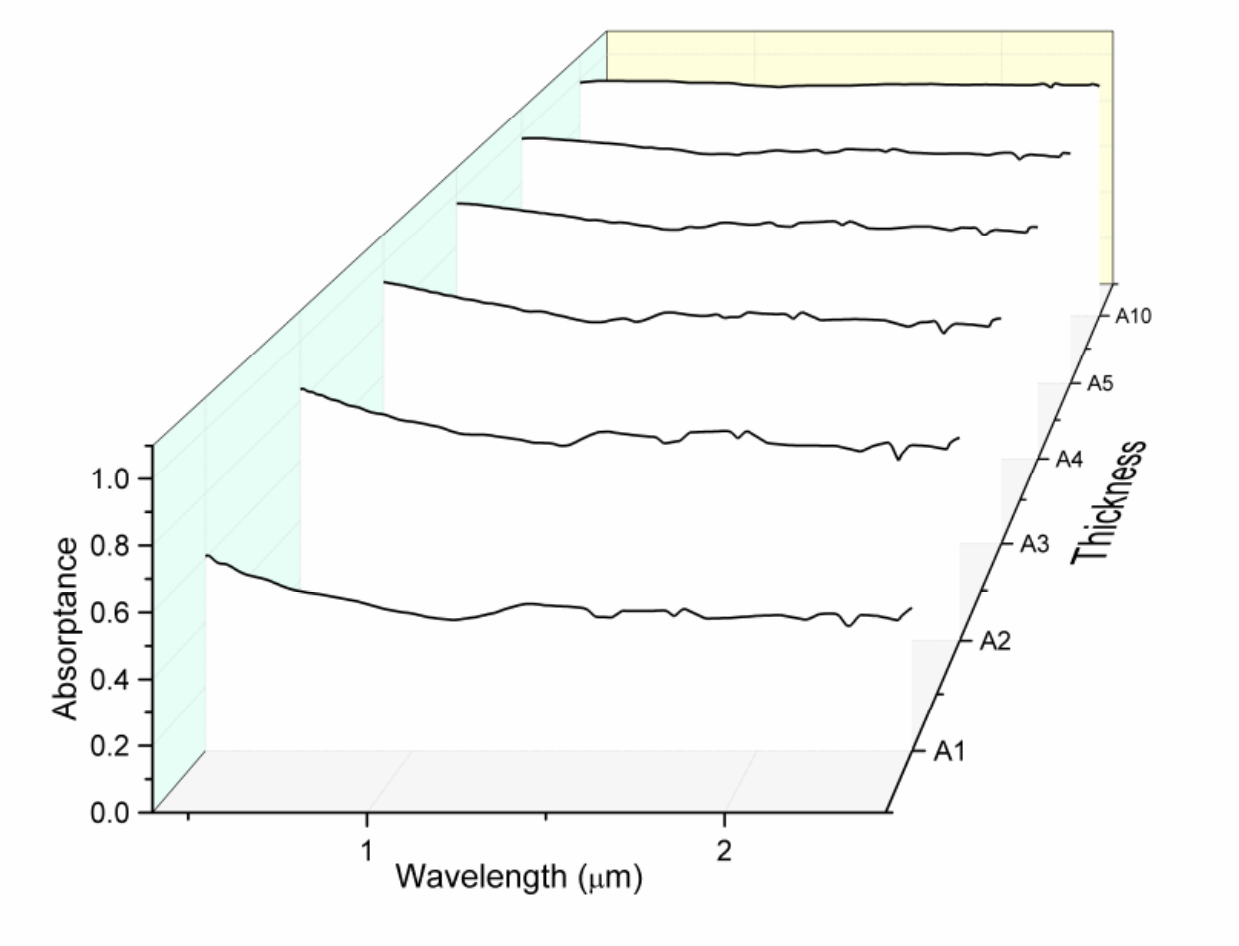


**Figure 5.7** Absorptance of BSi of different thicknesses: A1 - 1 μm, A2 - 2 μm, A3 - 3 μm, A4 – 4 μm, A5 – 5 μm, A10 – 10 μm as a function of wavelength [81].

The observation from Figure 5.7 is that the absorptance of B-Si increases with increase in thickness. The absorptance is close to unity as the thickness of B-Si is increased to 10 μm over the entire range of wavelength. The corresponding absorptance of B-Si, for various wavelengths and thicknesses, are presented in Table 5.1.

**Table 5.1** Absorptance Of BSi At Different Thicknesses And Wavelengths Obtained From Figure 5.7 [81].

| Wavelength(µm) | Thickness 1µm | Thickness 5µm | Thickness 10µm |
|---|---|---|---|
| **0.5** | 0.557 | 0.978 | 0.994 |
| **1.0** | 0.428 | 0.931 | 0.984 |
| **1.5** | 0.444 | 0.933 | 0.976 |
| **2.0** | 0.421 | 0.919 | 0.979 |
| **2.45** | 0.446 | 0.919 | 0.972 |

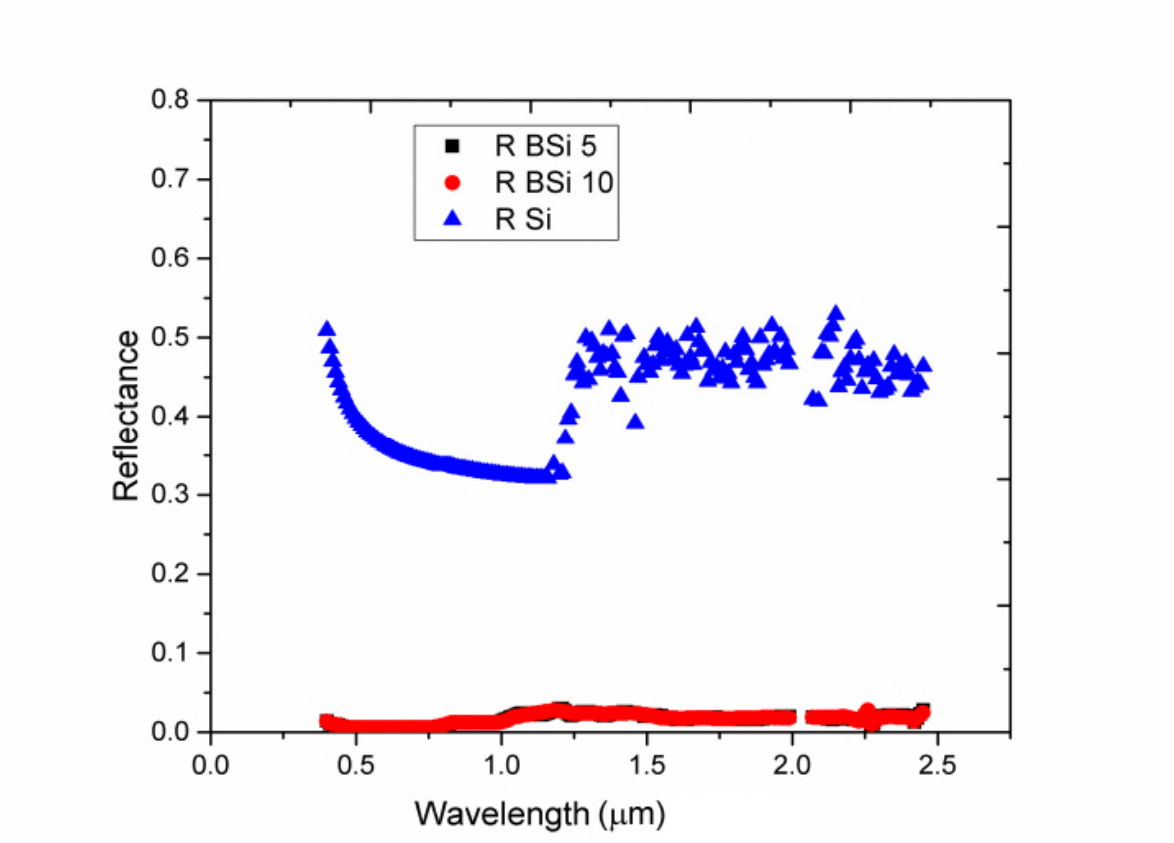


**Figure 5.8** Comparison plot of simulated reflectance of C-Si[29] and B-Si Of 5 µm and 10 µm thickness [81].

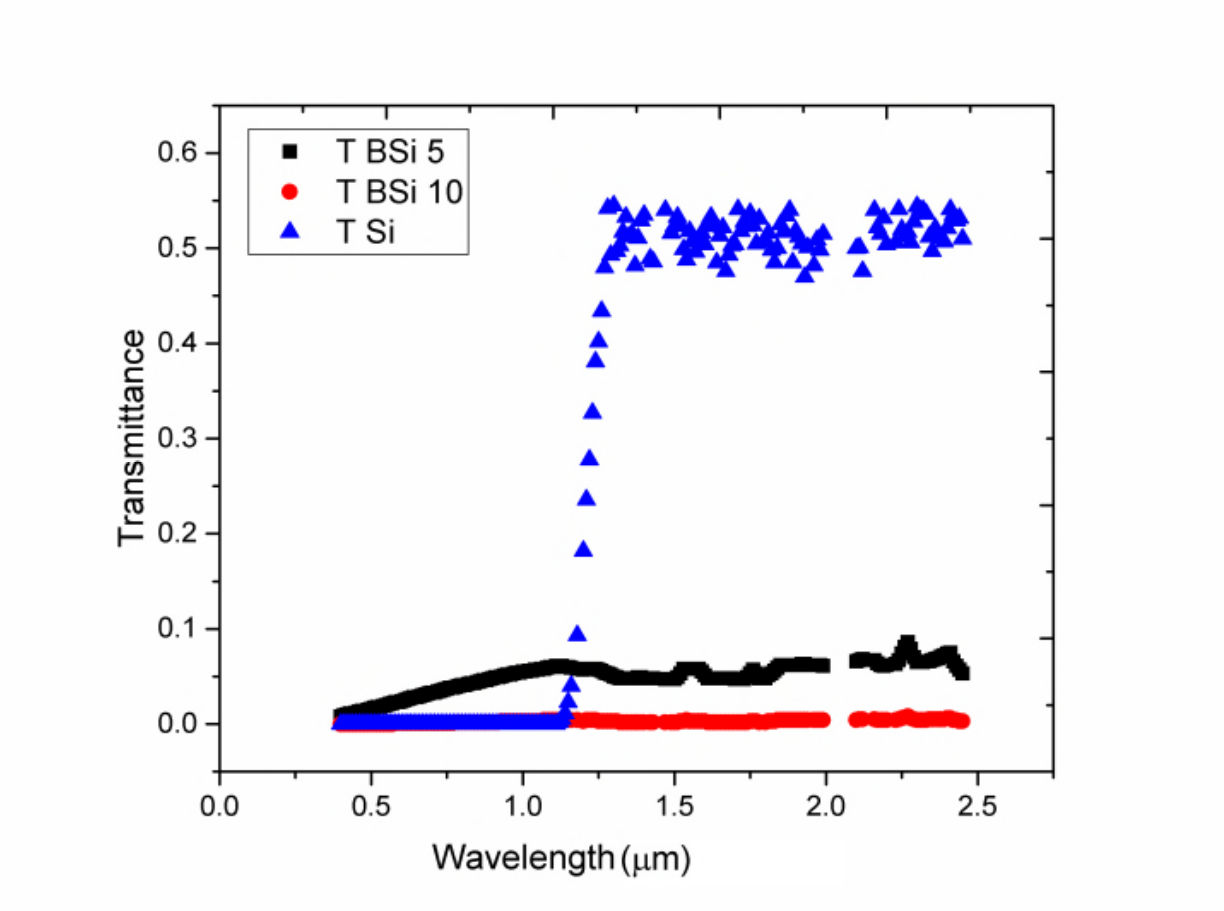


**Figure 5.9** Comparison plot of simulated transmittance of C-Si[29] and B-Si of 5 μm and 10 μm thickness [81].

The increase in R and T for Si around the wavelength of 1.1 μm, observed in Figures 5.8 and 5.9, corresponds to the energy gap of Si. There is a slight change in T of B-Si also in the same range of wavelengths. The difference in R and T of BSi and C-Si, and their dependence on wavelength and thickness, can be observed from Figures 5.8 and 5.9 respectively.

# CHAPTER 6

# APPLICATIONS AND FUTURE DIRECTIONS

## 1. Solar Cells

Solar energy is one of the most important renewable energy resources in the world. Among all kinds of solar cells, the fabrication technology of Silicon solar cells is relatively mature which makes them more popular in the solar cell market. However, in order to compete with the traditional energy sources, decreasing cost of per watt output seems necessary [56]. Hence, increasing the energy conversion efficiency with an economical approach is an unavoidable issue. One solution is applying anti-reflection layers onto the Silicon solar cells to maximize energy conversion efficiency. Black Silicon antireflection layers have attracted attention because their anti-reflection ability is less confined by the incident light angle and wavelength [70].

The crystalline Silicon wafers used to make today's solar cells are treated to create a textured surface, and then coated with an antireflective layer, usually Silicon nitride, using high-vacuum processes. This additional layer increases the value of a solar cell by improving its efficiency–it suppress reflection so that more photons actually enter the Silicon wafer instead of bouncing off its surface, increasing the flow of electricity off the cell. But the extra layer also adds to the expense. Black Silicon has been a subject of great interest in various fields including photovoltaics for its ability to reduce the surface reflectance even below 1 per cent [45- 47]. The most recent advancement took place in 2013 when the solar cell efficiency was calculated to be

18.7% by the Scientists at Aalto University, Finland and Fraunhofer ISE, Germany. The highest efficiency reported so far for a black Silicon solar cell [78].

The previous efficiency record of 18.2% was held by the U.S. Department of Energy's National Renewable Energy Laboratory (NREL) using thermal oxidation as a passivating layer [49].

Black Silicon solar cell future looks promising in the long run too. Branz's lab at the U.S. Department of Energy's National Renewable Energy Laboratory (NREL) is developing inexpensive ways to create black Silicon, which reflects almost no light. To replace the vacuum-deposition processes used to treat the surface of a Silicon wafer, Branz's lab [78] is developing a chemical process that can be performed at ambient temperature and pressure using equipment already on site at solar-panel factories. A wafer is submerged in a bath containing a water solution of hydrogen peroxide, hydrofluoric acid, and chloroauric acid, which is made up of hydrogen, chlorine, and gold. The small amount of gold in the acid bath acts as a catalyst for chemical reactions. It's not clear exactly what the chemical reactions will be, but they lead to the formation of gold nanoparticles that drill nanoholes at varying depths into the wafer. Also it is reported that the gold can be reused again and again [72-75].

**2. Image Sensing**

The SiOnyx proprietary Black Silicon laser process induces structural changes to detector materials [78]. This results in increased optoelectronic response in the visible and near infrared (NIR) regions. In addition, the spectral response is broadened, enabling Silicon

to respond further into the NIR [46]. These attributes have tangible value in most, if not all, photonic systems

SiOnyx XQE™ CMOS image sensors provide superior night vision, biometrics, eye-tracking, and natural human interface through our proprietary black Silicon semiconductor technology [46]. XQE image sensors deliver unprecedented performance advantages in infrared imaging, including sensitivity enhancements as high as 10x today's sensor solutions. Few of its properties include:

**Night Vision:**

- XQE enhanced IR sensitivity takes advantage of the naturally occurring IR 'nightglow' to enable imaging under extreme (<0.001 lux) conditions [62].

**Day/Night Surveillance:**

- XQE sensors provide high quality daytime color as well as nighttime imaging capabilities that offer new levels of performance and threat detection [62].

**Extended IR Imaging:**

- Systems that depend upon IR light to perform will be redefined by XQE sensor technology – from longer range covert IR illumination, to industrial IR sensing and range finding [77].

**Biometrics & Human Interfaces:**

- The enhanced IR sensitivity of XQE sensors enables higher performance and lower power IR based solutions at wavelengths >900nm [63].

### 3. Anti- Bacterial Surfaces

Black Silicon, a synthetic material studded with needle-shaped nanostructures that is used primarily for sensor applications, also serves as a potent antibacterial Agent, killing some 450,000 cells per minute in just one square centimeter [53]. Studies have shown that certain nanostructures can indeed kill based on texture alone. It had been previously demonstrated that cicada wings (*Psaltoda claripennis*) [4], which are covered in dense nanopillar structures, were highly lethal to the opportunistic human pathogen *Pseudomonas aeruginosa*, and provided evidence to suggest that the wings' biochemical properties were not responsible. It was proved that bactericidal nature of the wing is due to the mechanical rapture of bacterial cells according to the research [53].

Recognizing that dragonflies (*Diplacodes bipunctata*) also had similar nanopillars on their wings [7], and that Black Silicon was known for a similar nano-texture, researchers decided to explore the bactericidal potential of the two surfaces. Both caused significant deformation of the cell walls of *P. aeruginosa*, *Staphylococcus aureus*, and *Bacillus subtilis*, and even killed *B. subtilis* spores—at rates more than sufficient to stave off the bacteria [5, 7]. These provided potent bactericidal activity against not only Gram-negative bacteria but also against the more rigid and lysis-resistant Gram-positive bacteria and their spores.

The researchers at the Swinburne University of Technology in Australia have future plans to explore a range of other materials whose surfaces maybe suitable for fabrication similar structural nano-patterns to create surfaces free from bacteria [53].

# CHAPTER 7

# CONCLUSIONS

In physics, a black body is one that theoretically absorbs all incoming light. In reality, very few (if any at all) can achieve even remotely high retention rates that a theoretical black body can. Black Silicon is one of the few materials available that does retain the majority of incoming light, and with increased retention rates, black Silicon becomes significantly attractive for use in solar cells [68].

With the introduction of black Silicon, the absorption band widens and allows for absorption in the infrared region of the EM spectrum. This is achieved chiefly due to the presence of sulphur [3, 4]: the production of black Silicon uses sulfur hexafluoride gas and the sulfur atoms are forced to mix with the Silicon atoms on the surface, causing the band gap to be lowered. A lower band gap results in the ability to absorb longer wavelengths of the EM spectrum. This enables more light to be absorbed and less light wasted. In fact, compared to the Silicon used in solar cells, black Silicon is between 100 – 500 times more sensitive to insolation (due to its rough surfaces that catches light at all angles) and covers both the visible and infrared regions [72-77].

This increase in absorption has given rise to another feature: size. Silicon is expensive to purchase and process and Silicon is a material that is in relatively short supply. Having a material that increases absorption rates by up to 500 times [10, 13, 75] allows for thinner solar cells to be manufactured. Furthermore, as the manufacturing process for black Silicon is almost the same as for the manufacture of Silicon, no change

to the manufacturing process is required; in fact, the difference in cost is marginal and can be used with a conventional Silicon foundry.

One difference is that the black Silicon process requires a femtosecond laser to perform the etching, but the laser treatment actually can help reduce the manufacturing costs. The manufacturing costs are further reduced by the removal of the chemical processes typically used in the manufacture of Silicon-based solar cells [30, 70, 68].

"Silicon is known as an indirect absorber of light, which means that photons cannot be absorbed on their own, but must be assisted by a vibration of atoms within the material, which we call a phonon (rather than photon)," [62, 72, 73]. "On average, it takes hundreds of microns of thickness of Silicon to ensure that most photons will find a phonon and be absorbed. Black Silicon does not share this characteristic: all photons can be absorbed in the first few hundreds of nanometers (versus the first few hundreds of microns for standard Silicon)."

The solar industry has worked with anti-reflective treatments for a long time and many different approaches are being used. The basic approach of this thesis has been to develop a method that is **low-cost** and **applicable** to the existing Silicon solar cell production [80]. Most research is focused on creating the most optimal anti-reflective Black Silicon treatment possible, often reinventing much of the structure of the solar cell. Today many sophisticated anti-reflective treatments exist, but the high level of complexity of these technologies make them far too expensive to be applicable in the

market. Our approach does not signify reinventing the solar cell but rather focus on how to increase the absorption at a cheaper cost. The performance of the texturing method is very high despite the low cost, and it is the combination of cheap cost and high efficiency that makes Black Silicon unique [80].

## REFERENCES


1. Y. Xia, B. Liu, J. Liu, Z. Shen, C. Li, *A novel method to produce black Silicon for solar cells, Solar Energy* 85 (2011), pp. 1574–1578.

2. A. Balhamri, M. Rattal, Y. Bahou, A. Tabyaoui, M. Harmouchi, Az. Mouhsen and E. M. Oualim, *Black Silicon: Microfabrication Techniques and Characterization for Solar Cells Applications, International Journal of Energy Science (IJES),* (3) (6) (2013).

3. X. Liu, P. Coxon, M. Peters, B. Hoex, J. M. Cole and D. J. Fray, *Black Silicon: fabrication methods, properties and solar energy applications, Energy Environ. Sci*., (7) (2014), pp. 3223.

4. H. Su, J. Wu, Y. Lu, D. Flood, A. R. Barron, L. Chen, *Fabrication and characteristics of black Silicon for solar cell applications: An overview, Materials Science in Semiconductor Processing,* (25) (2) (2014), pp. 17.

5. Zhu, X. Zhang, H. Zhang, *Formation mechanism of multi-functional black Silicon based on optimized deep reactive ion etching technique with SF6/C4F8. Sci. China Tech Sci.*, (58) (2015), pp. 381-389.

6. H. Dekkers, F. Duerinckx, J. Szlufcik and J. Nijs, *Silicon surface texturing by reactive ion etching, Opto-Electronics Review,* (8) (4), (2000), pp. 311-316.

7. G. Kumaravelu, M. Malkaiii, A. Bittar , Surface Texturing For Silicon Solar Cells Using Reactive Ion Etching Technique, IEEE, (2002), pp. 7431-7803.

8. K. Nguyen, D. Saab, M. Malak, P. Basset, E. Richalot, N. Pavy, F. Flourens, F. Marty, D. Angelescu, Y. Leprince-Wang, T.Bourouina, *Study of Black Silicon Obtained by Deep Reactive Ion Etching – Approach to Achieving the Hot Spot of a Thermoelectric Energy Harvester, DTIP*, (2011).

9. T. Sarnet , M. Halbwax, R. Torres, P. Delaporte, M. Sentis, S. Martinuzzi, V. Vervisch, F. Torregrosa, H. Etienne, L. Roux, S. Bastide, *Femtosecond laser for black Silicon and photovoltaic cells, Proc. of SPIE*, (6881) (2008), pp. 688119.

10. C. Wu, *Femtosecond laser-gas-solid interactions,* Harvard University Cambridge, Massachusetts, (2000).

11. H. Alturaif, Z. Alothman, J. Shapter and S. Wabaidur, *Use of Carbon Nanotubes (CNTs) with Polymers in Solar Cells, Molecules* (*19* (2014), pp. 17329-17344.

12. Zeman, O. Isabella, K. Jäger, R. Santbergen, S. Solntsev, M. Topic and J. Krc, *Advanced Light ManAgement Approaches for Thin-Film Silicon Solar Cells, Energy Procedia,* (15) (2012), pp. 189 – 199.

13. V. Daudrix, J. Guillet, X. Niquille, A. Shah, Light trapping in amorphous Silicon solar cells, Commission for Technology and Innovation (CTI), (5810.1) (6315.1).

14. F. Flory , L. Escoubas , G. Berginc, *Optical properties of nanostructured materials: a review, J. Nanophoton,* (5) (1) (2011), pp. 052502.

15. M. Otto, M. Algasinger, H. Branz, B. Gesemann, T. Gimpel, K. Füchsel, T. Käsebier, S. Kontermann, S. Koynov, X. Li, V. Naumann, J. Oh, A. N. Sprafke, J. Ziegler ,M.Zilk, and Ralf, B. Wehrspohn, *Black Silicon Photovoltaics, Adv. Optical Mater.,* (3) (2015), pp. 147–164.

16. M. Steglich, T. Käsebier, M. Zilk, T. Pertsch, E.Kley, and A. Tünnermann, *The structural and optical properties of black Silicon by inductively coupled plasma reactive ion etching, Journal of Applied Physics,* (116) (2014), pp. 173503.

17. T. Sarnet, M. Halbwax, R. Torres, P. Delaporte, M. Sentis, S. Martinuzzi, V. Vervisch, F. Torregrosa, H. Etienne, L. Roux, S. Bastide, *Femtosecond laser for black Silicon and photovoltaic cells, Proc. of* SPIE, (6881), pp. 688119.

18. Wikipedia contributors, Crystalline Silicon, Wikipedia, The Free Encyclopedia, (2015).

19. Chemistry Explained, *Silicon, Advameg, (*2015), http://www.chemistryexplained.com/elements/P-T/Silicon.html, (Accessed on 01/21/2015).

20. L. Alchin, *The Periodic Table*, www.elementalmatter.info, (Accessed on 01/25/2015).

21. Bottyan, C. Rabago, *Chemistry of Silicon, http://chemwiki.ucdavis.edu/Inorganic_Chemistry/Descriptive_Chemistry/p-Block_Elements/Group_14%3A_The_Carbon_Family/Chemistry_of_Silicon* (Accessed on 02/2/2015).

22. International Energy Agency (IEA), "World Energy Statistics" (Organization for Economic Co-operation and Development, *Statistical Review of World Energy 2013*, Medium-Term Renewable Energy Market Report (2013), pp. 217.

23. M. Bollani, J. Osmond, G. Nicotra, C. Spinella and D. Narducci, *Strain-induced generation of Silicon nanopillars*, *Monica Bollani et al Nanotechnology*, (24) (2013), pp. 335302.

24. S. Cho, T. An and G. Lim, *Three-dimensionally designed anti-reflective Silicon surfaces for perfect absorption of light, Chem. Commun.,* (50) (2014), pp. 15710-15713.

25. *Anti-Reflection (AR) Coatings, Edmund Optics Inc.,* (2014), http://www.edmundoptics.com/technical-resources-center/optics/anti-reflection-coatings/, (Accessed on 01/10/2015).

26. D. Flood, *Black Silicon Antireflection Technology, Natcore Technology* (2004-2007), http://www.natcoresolar.com/. (Accessed on 01/19/2015).

27. T. Kim, H. Adeli, R. Robles, M. Balitanas, Advanced Communication and Networking: International Conference, Springer Science & Business Media, (2011), pp. 460-471.

28. E. Zhang, Z. Li, P. Li, Y. Shang, Y. Jia, J. Wei, K. Wang, H. Zhu, D. Wu, S. Zhang & A. Cao, *$TiO_2$- Coated Carbon Nanotube-Silicon Solar Cells with Efficiency of 15%*, 2 (884) (2002).

29. Y. Wang, Y. P. Liu, H. L. Liang, Z. X. Mei and X. L. Du, *Broadband antireflection on the Silicon surface realized by Ag nanoparticle-patterned black Silicon, Phys. Chem. Chem. Phys.,* (15) (2013), pp. 2345-2350.

30. M. Mayer, *Why Are Solar Cells Made Of Silicon?, Berkeley Energy and resources collaborative,* (2012), http://berc.berkeley.edu/why-are-solar-cells-made-of-silicon_1/ (Accessed on 01/16/2015).

31. T. Jefferson, National Accelerator Facility, *The Element Silicon,* http://education.jlab.org/faq/index.html (Accessed on 03/25/2015).

32. W. Haynes, ed., CRC Handbook of Chemistry and Physics, CRC Press/Taylor and Francis, Boca Raton, FL, 95th Edition, Internet Version 2015, accessed March 2015.

33. J. Emsley, *Nature's Building Blocks: An A-Z Guide to the Elements, Oxford University Press,* (2) (2011).

34. Krasnoshchekov, V.V. and LV Myshlyaeva, *Analtical Chemistry of Silicon, New York: Halsted Press*, (1974), pp. 1-6.

35. Rochow, G. Eugene, *Silicon and Silicones. New York: Springer-Verlag,* (1987), pp. 1-30.

36. Petrucci, H. Ralph, Harwood, S. William , F. Herring, and D. Madura, *"General Chemistry: Principles & Modern Applications."*, *Pearson Education*, (9) (2007).

37. M. Winter, *Web Elements: The periodic table*, www.webelements.com, (1993-2015)

38. R. Ritchie, *Failure of Silicon: Crack Formation and Propagation Crack Formation and Propagation,* Materials Sciences Division, Lawrence Berkeley National Laboratory, and Department of Materials Science and Engineering University of California, Berkeley, (2003).

39. *Properties of Silicon*, http://nautilus.fis.uc.pt/st2.5/scenes-e/elem/e01410.html (Accessed on 12/2/2015).

40. N. Winnie & Y. Xiong, *Review of Silicon photonics: history and recent advances, Journal of Modern Optics,* 60 (16) (2013), pp. 1299-1320.

41. Z. Li, *Czochralski Process , IEEE Trans Nucl. Sci.,* 39 (6) (1992), pp. 1730.

42. *Silicon Wafer Fabrication Process*, Department of computer and electrical engineering, Brigham Young University, (1994-Present).

43. L. Forbes, Historical Review, (1968-1969), http://doc.utwente.nl/38679/1/t0000018.pdf (Accessed on 14/2/2015).

44. H. Jansen, M. de Boer, R. Legtenberg, M. Elwenspoek, *"The black Silicon method: a universal method for determining the parameter setting of a fluorine-based reactive ion etcher in deep Silicon trench etching with profile control," Journal of Micromechanics and Microengineering ,* 5 (2), pp. 115.

45. M. Hidaka, *"Etching method (to avoid forming black Silicon)"*, United States Patent Application 20070167011, (2007)

46. V. Koifman, *THE HISTORY OF "BLACK SILICON" IN PHOTODETECTOR PATENTS*, (2012), http://image-sensors-world.blogspot.com/2012/12/the-history-of-black-Silicon-in_21.html (Accessed on 13/3/2015).

47. E. Niiler, *'Black' Silicon Grabs Infrared Sunlight*, (2012), http://news.discovery.com/tech/black-Silicon-solar-panels-121011.htm (Accessed on 19/3/2015).

48. M. Crawford, *Black Silicon is ready to revolutionize photo electronics*, *SPIE Newsroom*, (10) (2008), pp. 1117.

49. H. Jansen, H. Gardeniers, M. Boer, M. Elwenspoek and J. Fluitman, *A survey on the reactive ion etching of Silicon in microtechnology, J. Micromech. Microeng*., 6 (14) (1996), pp. 28.

50. J. Oh, H. Yuan and H. Branz, An 18.2%-efficient black-Silicon solar cell achieved through control of carrier recombination in nanostructures, NNANO, (2012), pp. 166.

*51.* R. Legtenberg, H. Jansen, M. Boer, and M. Elwenspoek, *Anisotriopic Reactive Ion Etching of Silicon Using SF6/O2/CHF3 Gas Mixtures, J. Electrochem. Sac.,* 142 (6) (1995).

52. Y. Huihui, J. Rui, C. Chen, D. Wuchang, W. Deqi, and L. Xinyu, *Antireflection properties and solar cell application of Silicon nanostructures, Journal of Semiconductors,* 32 ( 8) (2011).

53. S. Kalem, P. Werner, Ö. Arthursson, H. Frederiksen, V. Talalaev, U. Södervall, B. Nilsson, and M. Hagberg, *Black Silicon with high density and high aspect ratio nanowhiskers*, BMBF-TUBITAK bilateral program under contract No: 107T624.

54. E. Ivanova, J. Hasan, H. Webb, G. Gervinskas, S. Juodkazis, V. Truong, A. Wu, R. Lamb, V. Baulin, G. Watson, J.Watson, D. Mainwaring & R. Crawford, *Bactericidal activity of black Silicon, Nature Communications,* 4 (2013), pp. 2838.

55. S. Koynov, M.Brandt, and M. Stutzmann, *Black nonreflecting Silicon surfaces for solar cells, Applied Physics Letters,* (88) (2006), pp. 203107.

56. F. Semendy, P. Taylor, G. Meissner, and P. Wijewarnasuriya, *Black Silicon Germanium (SiGe) for Extended Wavelength Near Infrared Electro-optical Applications, ARL-TR-5202*, (2010).

57. J. Yoo, I. Parm, U. Gangopadhyay, K. Kim,S.K. Dhungel, D. Mangalaraj, J. Yi, *Black Silicon layer formation for application in solar cells, Solar Energy Materials & Solar Cells,* (90) (2006), pp. 3085–3093.

58. M. Stubenrauch, M. Fischer, C. Kremin, S. Stoebenau, A. Albrecht and O. Nagel, *Black Silicon—new functionalities in microsystems, J. Micromech. Microeng*. 16 (2006), pp. 82–87.

59. Z. Shen, B. Liu, Y. Xia, J. Liu, J. Liu, S. Zhong and C. Li, *Black Silicon on emitter diminishes the lateral electric field and enhances the blue response of a solar cell by optimizing depletion region uniformity, Scripta Materialia*, 68 (2013), pp. 199–202.

60. Zukauskas, M. Malinauskas, A. Kadys, G. Gervinskas, G. Seniutinas, S. Kandasamy, and S. Juodkazis, *Black Silicon: substrate for laser 3D micro/nano-polymerization, Optics Express 6901*, 21 (6) (2013).

61. H. Jansen, M. Boer, J. Burger, R. Legtenberg, and M. Elwenspoek, *The Black Silicon Method H: The Effect Of Mask Material And Loading On The Reactive Ion Etching Of Deep Silicon Trenches, Microelectronic Engineering,* 27 (1995), pp. 475480.

62. M. Otto , M. Kroll , T. Käsebier , S. Lee , M. Putkonen, R. Salzer , P. Miclea , and R. Wehrspohn*, Conformal Transparent Conducting Oxides on Black Silicon, Adv. Mater.*, (22) (2010), pp. 5035–5038.

63. Wang, H. Mei, S. Yin , J. Yao , C. Luo, Y. Chang, J. Cheng, Y. Zhu, *Development of novel flexible black Silicon, Optics Communications,* (284) (2011), pp. 1072–1075.

64. Vorobyev, C. Guo, *Direct creation of black Silicon using femtosecond laser pulses, Applied Surface Science,* (257) (2011), pp. 7291–7294.

65. P. Repo, A. Haarahiltunen, L. Sainiemi, M. Koski, H. Talvitie, M. Schubert, and H. Savin, *Effective Passivation of Black Silicon Surfaces by Atomic Layer Deposition, IEEE Journal Of Photovoltaics*, 3 (1) (2013).

66. H. Yuan, V. Yost, M. Page, P. Stradins, D. Meier, and H. Branz, *Efficient black Silicon solar cell with a density-graded nanoporous surface: Optical properties, performance limitations, and design rules, Applied Physics Letters* 95, (2009), pp. 123501.

67. H. Yuan, V. Yost, M. Page, L. Roybal, B. To, P. Stradins, D. Meier and H. Branz, *Efficient Black Silicon Solar Cells With Nanoporous Anti-Reflection Made In A Single-Step Liquid Etch*, *IEEE, 1 (9) (2009)*.

68. M. Barberoglou, V. Zorba, A. Pagozidis, C. Fotakis, and E. Stratakis, *Electrowetting Properties of Micro/Nanostructured Black Silicon, Langmuir* 26 (15) (2010), pp. 13007–13014.

69. S. Zhong, B. Liu, Y. Xia, J. Liu, J. Liu, Z. Shen, Z. X, and C. Li, *Influence of the texturing structure on the properties of black Silicon solar cell, Solar Energy Materials & Solar Cells*, 108 (2013), pp. 200–204.

70. Christiansen, J. Clausen, N. Mortensen, and A. Kristensen, *Minimizing scattering from antireflective surfaces replicated from low-aspect-ratio black Silicon, Applied Physics Letters* 101 (2012) pp. 131902.

71. F. Toor, H. Branz, M. Page, K. Jones, and H. Yuan, *Multi-scale surface texture to improve blue response of nanoporous black Silicon solar cells, Applied Physics Letters 99*, (2011), pp. 103501.

72. H. Branz, V. Yost, S. Ward, K. Jones, B. To, and P. Stradins, *Nanostructured black Silicon and the optical reflectance of graded-density surfaces, Applied Physics Letters 94*, (2009), pp. 231121.

73. L. Sainiemi ,V. Jokinen , A. Shah , M. Shpak , S. Aura , P. Suvanto ,and S. Franssila, *Non-Reflecting Silicon and Polymer Surfaces by Plasma Etching and Replication, Adv. Mater.*, (23) (2011), pp. 122–126.

74. M. Jones, S. Jones, *Optical Properties of Silicon,* http://www.univie.ac.at/photovoltaik/vorlesung/ss2014/unit4/optical_properties_Silicon.pdf, (Accessed on 03/25/2015).

75. L. Ma, Y. Zhou, N. Jiang, X. Lu, J. Shao, W. Lu, J. Ge, X. Ding, and X. Y. Hou, *Wide-band "black Silicon" based on porous Silicon, Applied Physics Letters 88*, (2006), pp. 171907.

76. Y. Xia, B. Liu, S. Zhong, and C. Li, *X-ray photoelectron spectroscopic studies of black Silicon for solar cell, Journal of Electron Spectroscopy and Related Phenomena*, 184 (2012), pp. 589–592.

77. Solar cells made from black Silicon, (2012), https://www.fraunhofer.de/en/press/research-news/2012/october/solar-cells-made-from-black-Silicon.html (Accessed on 02/16/2015).

78. M. Fischer, M. Stubenrauch, Th. Kups, H. Romanus, F. Morales, G. Ecke, M. Hoffmann, C. Knedlik, O. Ambacher and J. Pezoldt, *Self organization and properties of Black Self organization and properties of Black Silicon,* http://www.researchgate.net/publication/256938556_Self_organization_and_properties_of_Black_Silicon (Accessed on 02/21/2015).

79. N. Brown, *Black Silicon Solar Cell Efficiency Record Broken,* (2013), http://cleantechnica.com/2013/04/05/black-Silicon-solar-cell-efficiency-record-broken/ (Accessed on 03/19/2015).

80. Black Silicon Solar, http://www.blacksiliconsolar.com/technology.html, (Accessed on 4/29/2015).

81. S. Marthi, S. Sekhri and N. M. Ravindra, *Optical Properties of Black Silicon: An Analysis, JOM(The Journal of The Minerals, Metals & Materials Society (TMS))*- Communicated (2015).